RacGAP α2-chimaerin adjusts spine morphological features and cognitive ability

Ryohei Iwata

Doctor of Philosophy

Department of genetics

School of life science

The Graduate University for Advanced Studies (SOKENDAI)

Department of Developmental Genetics

National Institute of Genetics

2013

The Contents of the Doctoral Thesis

ABBREVIATIONS

α1α2-C: α-chimaerin-isoform-common-C-terminus

α1KO: α1-isoform-specific α-chimaerin knockout

α2KO: α2-isoform-specific α-chimaerin knockout

aa: amino acid

αChn: α-chimaerin

αChnKO: α-chimaerin knockout

Ab: antibody

Ad: adult

Ad-α2KO: adult-specific α2-isoform α-chimaerin knockout

Ad-αChnKO: adult-specific α-chimaerin knockout

AMPA: alpha-amino-3-hydroxy-5-methyl-4-isoxazole propinate

ASD: autism spectrum disorder

C1: protein kinase C1 conserved region 1

CDS: coding region

CPG: central pattern generator

CS: conditioned stimulus

CST: corticospinal tract

Da: dalton

DAG: diacylglycerol

DAPI: 4',6-diamidino-2-phenylindole

dB: decibel

DG: dentate gyrus

DiI: 1,1'-dioctadecyl-3,3,3',3'-tetramethylindocarbocyanine perchorate

DIV: days in vitro

DT: dorsal telencephalon

DT-α1KO: dorsal telencephalon-specific α1-isoform α-chimaerin knockout

DT-α2KO: dorsal telencephalon-specific α2-isoform α-chimaerin knockout

DT-αChnKO: dorsal telencephalon-specific α-chimaerin knockout

E: embryonic day

fEPSP: field excitatory postsynaptic potential

FV: fiver volley

Hz: hertz

KLH: keyhole-limpet hemocyanin

KO: knockout

LTP: long-term potentiation

mAb: monoclonal antibody

NGS: normal goat serum

NS: non significant

OE: overexpression

P: postnatal day

pAb: polyclonal antibody

PB: phosphate buffer

PBS: phosphate buffered saline

PCR: polymerase chain reaction

PFA: paraformaldehyde

PSD: postsynaptic density

RacGAP: Rac GTPase activating protein

RacGEF: Rac guanine nucleotide exchange factor

SEM: standard error of the mean

SH2: src homology 2

TAM: tamoxifen

TBS: theta-burst stimulation

US: unconditioned stimulus

WT: wild-time

INTRODUCTION

In the mammalian brain, most excitatory synapses are formed on small protrusions of the dendritic membrane known as dendritic spines (Nimchinsky et al., 2002). Spine morphological characteristics (e.g., size and density) are fundamental to synaptic function (Bourne and Harris, 2008; Kasai et al., 2010). For example, the spine volume correlates with the area of the postsynaptic density (PSD) and strength of the synapse. The spine length is proportional to the extent of biochemical and electrical isolation from the dendritic shaft. The spine density indicates the number of excitatory synaptic inputs they receive. Dendritic spines are highly dynamic and continuously change their size and number positively and negatively from the putative "baseline" in response to a variety of stimuli, such as those derived from cell-to-cell communication and synaptic activity (Bourne and Harris, 2008). Adult spine remodeling is well-recognized as the morphological basis of neural circuit remodeling underlying brain functions including learning and memory (Holtmaat and Svoboda, 2009; Yuste and Bonhoeffer, 2001). Recent evidence, using animal models of neurodevelopmental disorders such as autism spectrum disorders (ASDs) and schizophrenia, identifies several genes whose malfunction is associated with an abnormality in spine morphogenesis and impairment of adult brain function (Bagni and Greenough, 2005; Cahill et al., 2009; Clement et al., 2012), suggesting that spine morphogenesis during development may somehow impact on cognitive ability in adulthood (Penzes et al., 2011). However, it remains unclear whether and how the baseline of spine morphological features in adulthood, which underlie cognitive ability, is determined during development.

The morphological changes of dendritic spines heavily depend on actin cytoskeleton remodeling by Rho-family small GTPases, such as RhoA, Rac, and Cdc42 (Ethell and Pasquale, 2005) both during development and in adulthood. α-chimaerin (α-chimerin) is a Rac-specific

GTPase-activating protein (RacGAP), which is a negative regulator of Rac activity (Diekmann et al., 1991; Hall et al., 1990; Hall et al., 1993). α-chimaerin is composed of α1- and α2-isoforms, generated as alternatively spliced products (Dong et al., 1995; Hall et al., 1990; Hall et al., 1993), which are expressed specifically in the central nervous system. The expression of the α1-isoform is high in adulthood, whereas the expression of the α2-isoform is high during development (Hall et al., 2001; Lim et al., 1992). Studies in a newly discovered spontaneous *α-chimaerin* null mutant mouse, named *miffy* mouse, and an α-chimaerin knockout (KO) mouse, has revealed an *in vivo* function for α-chimaerin; α2-chimaerin regulates midline axon guidance of the corticospinal tract (CST) and central pattern generator (CPG) as a key mediator of ephrinB3/EphA4 forward-signaling, and its loss-of-function results in hopping gaits in the animals (Iwasato et al., 2007). Subsequently, three other groups reported similar results using different sets of KO mice (Beg et al., 2007; Wegmeyer et al., 2007), or by an *in vitro* study (Shi et al., 2007). A recent study using a knockdown approach suggests a role for α2-chimaerin in cortical neuron migration, albeit in a RacGAP-independent manner (Ip et al., 2012). In humans, gain-of-function mutations of the α-*chimaerin* gene *CHN1* cause Duane's retraction syndrome, an eye movement disorder caused by the disruption of axon guidance in the ocular motor system (Miyake et al., 2008). These reports suggest important roles for RacGAP α2-chimaerin in axon guidance. In addition, RacGAP α2-chimaerin may contribute to spine remodeling, since α2-chimaerin protein is present not only in the axonal growth cone, but also in the dendritic spine (Iwasato et al., 2007; Shi et al., 2007). However, at present, there are no reports of the involvement of α2-chimaerin in dendritic spine function. Furthermore, the contributions of α2-chimaerin to higher brain functions remain to be explored.

By analyzing a series of global and conditional KO mice of α-chimaerin and its isoforms, I revealed that α-chimaerin has a wide variety of roles in brain function and that α1-

and α2-isoforms have distinct roles *in vivo*. Especially, a role of α2-chimaerin in the hippocmapus is important. Deletion of α2-chimaerin from the developmental stages, but not in adulthood, results in an increase in the size and density of hippocampal spines in adulthood, and an increase in hippocampus-dependent learning in adult mice. *In vitro* studies also revealed that α2-chimaerin plays a role in the spine retraction process by mediating ephrinA/EphA forward-signaling in hippocampal neurons during development. Taken together, my results suggest that during development, α2-chimaerin negatively regulates spine remodeling to adjust the morphological features of dendritic spines (size and density) of adult hippocampal neurons, and thereby determine the ability for hippocampus-dependent learning.

RESULTS

A variety of behavioral abnormalities in global αChn-deficient mice

Previously, it was discovered that a spontaneous recessive mutation of the *α-chimaerin* gene (*Chn1*) in *Miffy* mutant (*Chn1*$^{mfy/mfy}$) mice manifested phenotypes such as a rabbit-like hopping gait and impaired midline axon guidance of the CST and spinal CPG (Iwasato et al., 2007). To investigate the roles of α-chimaerin in the broader aspects of neural circuit function and animal behavior, I performed a comprehensive behavioral test on α-chimaerin (αChn)-deficient mice (*Chn1*$^{mfy/mfy}$ or *Chn1*$^{-/-}$ = αChnKO mice) and their littermate controls (*Chn1*$^{mfy/+}$ or *Chn1*$^{+/-}$, respectively)(Figure 1). Besides the rabbit-like hopping gait, αChn-deficient mice exhibited abnormalities in various behavioral tests (Figures 2 and S1, and Table S1). A striking phenotype was their extremely high levels of locomotor activity: they showed about four times and eighteen times higher locomotor activity than the control mice in the open field test (Figure S1A) and homecage activity test (Figure S1B), respectively. Another important phenotype was observed in the contextual fear learning test (Figure 2A(a)): the fear conditioning tests were applied to assess the subjects' learning and memory abilities (LeDoux, 2000). In these tests, αChnKO mice showed normal 'freezing' levels in the conditioning phase (data not shown) and cued test (Figure 2A(a)). On the other hand, in the contextual test, which is a hippocampus-dependent task (Kim and Fanselow, 1992; Phillips and LeDoux, 1992), αChnKO mice showed increased 'freezing' compared to the controls (Figure 2A(a)), indicating better contextual fear memory in these mice. In the following studies, I primarily focused on contextual fear conditioning and other types of hippocampus-dependent learning.

An increase in contextual fear learning in DT-αChnKO mice

Since global αChn-deficient mice showed abnormalities in various behavioral paradigms (Table

S1), it was not clear whether the increase in the contextual fear learning phenotype was ascribed to the direct effects of the α-chimaerin disruption, or was merely a consequence of other behavioral abnormalities such as locomotor hyperactivity and hopping gait. To distinguish between these two possibilities, region-specific αChnKO mice were generated using the Cre/loxP system (Figure 1A). I crossed αChn-flox mice with Emx1-Cre knock-in mice, which show Cre-mediated recombination in all excitatory neurons of the dorsal telencephalon (DT), including the hippocampus and cerebral cortex from the embryonic stages (Iwasato et al., 2000; Iwasato et al., 2008), to generate DT-specific αChnKO (DT-αChnKO = $Emx1^{Cre/+}$;$Chn1^{flox/-}$) mice. I performed a series of behavioral tests of the DT-αChnKO mice and their littermate controls ($Chn1^{flox/-}$). Although the DT-αChnKO mice behaved normally in most behavioral paradigms (Figures S1D and S1E and Table S1), they exhibited an increase in contextual fear learning behavior similar to that observed in the global αChnKO mice (compare Figures 2A(a) and 2A(b)). These results demonstrate that an increase in contextual fear memory was caused by the direct effects of a loss of α-chimaerin in the excitatory neurons of the DT (such as hippocampus).

The α2, not α1, isoform regulates hippocampus-dependent learning

α1- and α2-chimaerin show different biochemical properties *in vitro* and they have spatially and temporally distinct expression patterns in the mouse brain (Buttery et al., 2006; Hall et al., 2001; Lim et al., 1992). To test if these two isoforms have distinct functions *in vivo*, isoform-specific flox mice and KO mice were generated (Figure 1A) and I subjected the isoform-specific KO mice to a series of behavioral tests. The α2-isoform-specific KO (α2KO)($Chn1^{\Delta\alpha2/\Delta\alpha2}$) mice showed similar phenotypes to the αChn-deficient mice, in which both α1- and α2-isoforms were disrupted (Figures 2A(d), S1I and S1J, and Table S1). On the other hand, the

α1-isoform-specific KO (α1KO)(*Chn1*$^{\Delta\alpha1/\Delta\alpha1}$) mice showed distinct behavioral phenotypes (Figures 2A(c) and S1F-S1H, and Table S1): for instance, in the elevated plus maze test, the α1KO mice displayed increased anxiety-like behavior (Figure S1H), whereas α2KO mice displayed decreased anxiety-like behavior (Figure S1J). These results indicate that the α1- and α2-isoforms play distinct roles in brain function.

In the fear conditioning test, the α1KO mice showed normal fear memory in both cued and contextual tests when compared to their controls (*Chn1*$^{+/+}$, Figure 2A(c)). On the other hand, both α2KO mice and DT-specific α2KO (DT-α2KO = *Emx1*$^{Cre/+}$;*Chn1*$^{\alpha2flox/-}$) mice showed an increase in contextual fear memory when compared to their controls (*Chn1*$^{\Delta\alpha2/+}$ and *Chn1*$^{\alpha2flox/-}$, respectively, Figures 2A(d) and 2A(e)). I then assessed spatial memory, which is also hippocampus-dependent, in the α2KO mice using an automated monitoring system for mouse behavior in a social context, named the "IntelliCage" system (Krackow et al., 2010; Voikar et al., 2010). In the avoidance learning test, water is available for the mice to drink in all four corners of the cage; however, one corner is designated as the air-punishment corner. The α2KO mice displayed a higher percentage of "Visit Avoidance" to the air-punishment corner in the probe trial compared to the control (Figure 2C(a)), indicating that hippocampus-dependent avoidance memory is also increased in α2KO mice. On the other hand, extinction learning is not altered between genotypes (Figure 2C(b)). In the place preference test, mice were able to drink water in only one corner, whereas in the reversal learning test, water was available only in the opposite corner (Figure 2D(a)). The α2KO mice showed a higher place preference (Figure 2D(b)) and reversal learning (Figure 2D(c)) compared to the control mice, although the difference was not significant. Thus, the α2KO mice showed better hippocampus-dependent learning not only in contextual fear learning, but also in spatial avoidance learning in the IntelliCage system.

A developmental role for α2-chimaerin in contextual fear learning

Since gene disruption occurs from the early developmental stages in both the α2KO and the DT-α2KO mice, it is important to determine which of during development, or in adulthood, α2-chimaerin is involved in the negative regulation of hippocampus-dependent learning. The temporal expression patterns of α2-chimaerin show higher expression during development than in adulthood (Figure S4)(Buttery et al., 2006; Hall et al., 2001), which suggests that α2-chimaerin plays a role in development. To confirm this, I generated temporally-controlled α2KO mice. I crossed α2-flox mice with SLICK-H transgenic mice, which robustly express CreERT2 recombinase in the widespread brain (Heimer-McGinn and Young, 2011; Young et al., 2008), to obtain *SLICK-H*;*Chn1*$^{\alpha 2flox/-}$ mice. Tamoxifen was administered to 1-month-old *SLICK-H*;*Chn1*$^{\alpha 2flox/-}$ mice for 10 days (see Extended Experimental Procedures), and referred to as Adult-specific α2KO (Ad-α2KO) mice. The fear conditioning test was performed 1 month after the last tamoxifen administration; at this stage α2-chimaerin protein was barely detectable in the Ad-α2KO hippocampus (Figure S2). However, in contrast to the α2KO mice and DT-α2KO mice, which showed an increase in contextual fear memory, Ad-α2KO mice showed normal fear memory in both the cued and contextual tests, when compared to their littermate controls (tamoxifen-treated *SLICK-H*;*Chn1*$^{\alpha 2flox/+}$)(Figures 2A(d)-2A(f)). In addition, I generated adult-specific αChnKO (Ad-αChnKO = tamoxifen-treated *SLICK-H*;*Chn1*$^{flox/-}$) mice and demonstrated that they also showed normal fear memory (data not shown). These results suggest that α2-chimaerin is involved in contextual fear learning in the developing brain, and not in the adult brain. Taken together, my findings (Figure 2) revealed that α2-chimaerin acts in the DT during development, and establishes normal hippocampus-dependent learning ability in adulthood.

A developmental role for α2-chimaerin in dendritic spine morphogenesis

To identify hippocampus subregion(s) which may be responsible for increased contextual fear learning in α-chimaerin-deficient mice, I quantitatively analyzed neuronal activity levels in the hippocampal CA1, CA3 and dentate gyrus (DG) of DT-αChnKO mice, in the presence and absence of fear conditioning. Neuronal activity levels were compared, between genotypes, by immunohistochemistry of an immediate early gene c-Fos (Beck and Fibiger, 1995). In the CA1 region, the c-Fos expression level after fear conditioning, but not in homecage, was significantly lower in DT-αChnKO mice than in control mice (Figure S3). These differences were not observed in hippocampal CA3 and DG (data not shown), suggesting that the CA1 may be the most important site, in the hippocampus, where α2-chimaerin functions for suppression of contextual fear learning.

α2-chimaerin is a Rac-specific inactivator; Rac is a key regulator of actin cytoskeleton remodeling, which is associated with the formation of axonal projections and dendritic spine morphogenesis in developing neurons. α2-chimaerin is found in both axonal growth cones and dendritic spines (Iwasato et al., 2007; Shi et al., 2007). Therefore, it is possible to assume that α2-chimaerin-deficient mice may have abnormalities in their axonal projections, and/or dendritic spine morphogenesis in the developing hippocampus and that these abnormalities may underlie the increase in hippocampus-dependent learning in these mice in adulthood. To identify such morphological changes, I analyzed the hippocampus of the DT-α2KO mice. The gross morphology of the DT-α2KO hippocampus was normal (data not shown), and is consistent with a previous report of the normal gross morphology of the αChn-deficient mouse brain (Iwasato et al., 2007). I examined axonal projection patterns of the hippocampus, by immunostaining with the pathway-specific axonal markers, netrin-G1 and netrin-G2 (Nishimura-Akiyoshi et al., 2007), to visualize the laminar structures of the hippocampus; I found that the gross axonal projection

was normal in the adult DT-α2KO mouse hippocampus (Figure S5). In addition, I have not found significant differences in dendrite morphology and complexity of hippocampal CA1 pyramidal neurons from adult DT-α2KO mice, compared with the control mice (Figure S6).

I then focused on dendritic spine structures. Immunohistochemistry revealed that, in the hippocampus during development (for example, at postnatal day 14 (P14)), α2-chimaerin expression levels were highest in the stratum radiatum, the pyramidal layer and the stratum oriens of the CA1 region (Figure S4); these contained apical dendrites, cell bodies, and basal dendrites, respectively. I labeled the CA1 hippocampal spines and analyzed their morphology at the juvenile stage (Figures 3A, 3B(a) and S7). Spines in apical dendrites, but not basal dendrites, of the hippocampal CA1 in The DT-α2KO mice, were significantly longer and larger than those of control mice (Figures 3B(a) and S7). This apical dendrite-specific spine enlargement was also observed in adult DT-α2KO mice (Figure 3B(b)). These results suggest that α2-chimaerin contributes as a suppressor of dendritic spine enlargement during development.

In the mouse forebrain, the number of dendritic spines increases until about 4-week-old, and then decreases until adulthood (developmental spine loss)(Nimchinsky et al., 2001; Zuo et al., 2005). Juvenile DT-α2KO mice showed normal spine densities along apical dendrites of CA1 neurons (Figure 3B(a)). On the other hand, adult DT-α2KO mice showed higher spine density than control mice (Figure 3B(b)), and the developmental spine loss was suppressed in DT-α2KO mice (Figure 3C). These results suggest that α2-chimaerin mediates the spine elimination process and/or the suppression of spine formation process during development. Since previous studies have suggested that (1) overexpression or knockdown of α1-chimaerin affects spine morphology in cultured hippocampal neurons (Buttery et al., 2006; Van de Ven et al., 2005), and (2) α1-chimaerin is highly expressed in the adult hippocampus (Hall et al., 2001), I next examined whether deletion of α1-chimaerin alters spine morphology *in vivo*. Adult

DT-α1KO mice showed normal spine size and density of hippocampal CA1 pyramidal neurons compared to control mice (Figure 3B(c)). These results indicate that deletion of α2-isoform of α-chimaerin, not α1-isofrom, affects hippocampal spine morphology *in vivo*.

Next, I analyzed the spine morphological phenotypes of adult Ad-α2KO mice to confirm that loss of α2-chimaerin during development contributes to the enlarged size and increased densities of the dendritic spines in the DT-α2KO mouse spines. In the Ad-α2KO mice, although the volume of the apical dendrite spines increased, the length decreased (Figure 3B(d)). The Ad-α2KO mice also showed a decrease in spine density, although the difference was not significant (Figure 3B(d)). These dendritic spine phenotypes of the Ad-α2KO mice were very different to those of the DT-α2KO mice in adulthood (Figure 3B(b)), indicating that α2-chimaerin during development plays an important role in determining dendritic spine morphology (e.g., size and density) in adulthood.

I examined whether dendritic spine alterations in the DT-α2KO mouse hippocampus affect synaptic functions in adulthood by evaluating the strength of the CA3-CA1 synapses of the stratum radiatum in hippocampal slices. I found that the field excitatory postsynaptic potential (fEPSP) slopes, but not fiber volley (FV) amplitude, were significantly increased in the DT-α2KO mice compared to those of the control mice (Figure S8A), suggesting that basal synaptic transmission was increased in the adult DT-α2KO mice. It is likely that the increased transmission is attributed to an increased responsiveness of postsynaptic neurons (over entire apical dendrite) to released glutamate, because there was no difference in the ratio of paired-pulse facilitation (Figure S8B). Whereas theta-burst stimulation (TBS)-induced long-term potentiation (LTP) was not altered between the DT-α2KO and the control mice (Figure S8C). These results suggest that α2-chimaerin negatively regulated basal synaptic transmission, but had no effect on LTP in the hippocampus.

RacGAP activity of α2-chimaerin regulates dendritic spine size in the developing hippocampus through cell-autonomous mechanisms

To obtain further insight into the mechanisms by which α2-chimaerin plays a role in spine morphogenesis, I performed single-cell overexpression experiments (see Experimental Procedures). The overexpression of α2-chimaerin (α2(WT)OE) in the hippocampal pyramidal neurons of juvenile wild-type mice decreased spine length and volume but not density, when compared with the control neurons (Figure 4B). On the other hand, overexpression of the GAP-inactive mutant of α2-chimaerin (α2(R304G)OE)(Hall et al., 2001) did not alter spine size, when compared with the control neurons (Figure 4B). These results suggest that RacGAP activity of α2-chimaerin is required for the negative regulation of dendritic spine size in hippocampal neurons during brain development. These data also demonstrated that overexpression of α2-chimaerin affects spine morphology through cell-autonomous mechanisms, because in these experiments, overexpression was induced only in a sparse population of neurons in the CA1 region (Figure S9B).

Both α1- and α2-isoforms contain C1 and RacGAP domains in their C-terminal. α1-chimaerin has a relatively short N-terminal that does not contain any recognizable domains, whereas α2-chimaerin has an SH2 domain in its N-terminal (Figure S9A). To examine the importance of the α2-specific N-terminus in spine morphogenesis, I performed single-cell overexpression experiments using wild-type α1-chimaerin (α1-chimaerin(WT)) and the isoform-common-C-terminal (α1α2-C(WT))(Figure S9A). I found that the migration of the hippocampal cells was drastically impaired when either α1-chimaerin(WT) or α1α2-C(WT) was overexpressed (Figure S9B). I did not observe the abnormal cell migration when I overexpressed Rac-inactive α1-chimaerin(R304G), α1α2-C(R304G), or α2-chimaerin(WT or R304G). These

results suggest that α-chimaerin has the ability to suppress cell migration in a RacGAP-dependent manner; while this ability is tightly inhibited in α2-chimaerin by its N-terminus. The present study data are consistent with those from previous *in vitro* studies showing that the α2-chimaerin-specific N-terminal is an autoinhibitory region that inhibits RacGAP function through its occlusion of the C1 and GAP domains when the molecule is inactive (Canagarajah et al., 2004; Colon-Gonzalez et al., 2008). Thus, although dendritic spine analyses were hampered by unexpected cell migration defects, the overexpression experiments of α1-chimaerin or α1α2-C provided *in vivo* evidence for the importance of the α2-chimaerin-specific N-terminus in the regulation of the RacGAP activity of α-chimaerin.

The deletion of α2-chimaerin suppresses ephrinA-induced spine retraction

I next determined the upstream signaling molecule(s) involved in α2-chimaerin-dependent spine morphogenesis. It is known that in the midline guidance of the CST and CPG axons, α2-chimaerin mediates ephrinB3/EphA4 forward-signaling (Beg et al., 2007; Iwasato et al., 2007; Wegmeyer et al., 2007). At the CA1 apical dendritic synapses, ephrinA3, which is localized in the astrocytic processes near the spines, activates EphA4, which is enriched in dendritic spines, to induce the spine retraction process (Carmona et al., 2009; Klein, 2009; Murai et al., 2003). EphA4KO mice show increased spine size and density in the apical dendrites of CA1 pyramidal neurons (Murai et al., 2003), which are similar to those observed in the DT-α2KO mice (Figure 3). EphrinA3KO mice also display increased spine size in the apical dendrites of CA1 pyramidal neurons (Carmona et al., 2009). Therefore, I hypothesized that ephrinA3/EphA4 forward-signaling may contribute to α2-chimaerin-dependent spine morphogenesis. To test this hypothesis, I performed a spine retraction assay using hippocampal slice cultures, in which pyramidal neurons were sparsely labeled. Hippocampal slice were

prepared from P5 mice, cultured for six days, and were treated with pre-clustered ephrinA3-Fc (Figure 5). Consistent with previous reports (Fu et al., 2007), ephrinA stimulation induced a reduction in spine numbers (Figure 5C). By contrast, ephrinA3-induced spine retraction was suppressed in α2KO mouse neurons (Figure 5C). These results support my hypothesis that α2-chimaerin acts as a downstream effector of ephrinA3/EphA4 forward-signaling in spine morphogenesis in the developing hippocampus.

DISCUSSION

α2-chimaerin in development establishes normal spine morphological features in adulthood and hippocampus-dependent learning

In this study, I have shown the following: (1) Hippocampus-dependent learning, such as contextual fear learning, increases in mice which lack the α2-isoform of α-chimaerin in the hippocampus from the developmental stage (αChnKO, DT-αChnKO, α2KO and DT-α2KO mice), but not in α1KO or Ad-α2KO mice (Figure 2); (2) Increases in dendritic spine size and density are observed in the DT-α2KO, but not in the DT-α1KO and Ad-α2KO mouse hippocampus (Figure 3); (3) Overexpression of α2-chimaerin induces a decrease in dendritic spine size in the developing hippocampus via a RacGAP activity-dependent and cell-autonomous mechanism (Figure 4); (4) Basal synaptic transmission, but not LTP, increases in the adult DT-α2KO mouse hippocampus (Figure S8); and (5) EphrinA-induced spine retraction in the developing hippocampal slice culture, which depends on EphA4 expression (Fu et al., 2007), is suppressed in α2KO mouse (Figure 5). Taken together, these results suggest that RacGAP α2-chimaerin mediates ephrinA/EphA forward-signaling during development to establish the normal size and density of hippocampal spines in adulthood, which corresponds to normal levels of hippocampus-dependent learning and memory (Figure 6).

The balance between RacGAP and RacGEF activities during development may adjust the "baseline and framework" of the spine morphological characteristics, which defines cognitive ability in adulthood

The morphological characteristics of dendritic spines (e.g., size and density) are fundamental to synaptic function (Bourne and Harris, 2008; Kasai et al., 2010). Spines are highly dynamic and continuously change their size and density positively and negatively from a putative baseline, in

response to a variety of stimuli (Bourne and Harris, 2008). Thus, the baseline of the spine morphological features in adulthood could define the basal ability of synaptic function underlying the cognitive ability of individuals; when the baseline is high and low, cognitive ability should also be high and low, respectively. However, it is not clear how the baseline of the spine morphological features in adulthood is determined.

My results suggest that RacGAP α2-chimaerin during development contributes to the adjustment of the spine morphological baseline in adulthood, by negatively regulating Rac levels during development (Figure S10). Rac activity is determined by the balance of positive and negative regulation by Rac guanine nucleotide exchange factors (RacGEFs) and RacGAPs, respectively. Therefore, there may be specific RacGEFs that have opposite functions to RacGAP α2-chimaerin in the determination of the spine morphological baseline. RacGEF kalirin-7 is a candidate for this role: the global KO mice of kalirin-7 show reduced Rac activity, decreased spine size and density, and impaired learning and memory (Cahill et al., 2009; Ma et al., 2008); the kalirin-7 KO mice also show exaggerated developmental spine loss (Cahill et al., 2009). The phenotypes of the kalirin-7 KO mice are opposite to those of the α2-chimaerin-deficient mice. Further studies such as those using conditional KO mice are required to elucidate the roles of kalirin-7 during development, and in adulthood. I hereby propose a model for the baseline of the morphological features of the dendritic spines (e.g., size and density) in adulthood, which underlie cognitive ability, that is at least partly determined by the balance between positive and negative regulation of Rac activity by specific RacGEFs (e.g., kalirin-7) and RacGAPs (e.g., α2-chimaerin), respectively, during development (Figure S10); when the balance is shifted to either direction by the absence of RacGEFs or RacGAPs during development, the baseline may also be shifted, which should result in an altered cognitive ability.

My model may also provide an important insight into how humans have evolved to

acquire intelligence. Dendritic spines in human are longer, lager and more densely packed than those of the mouse (Benavides-Piccione et al., 2002), suggesting that the spine morphological baseline and framework are different between species, and is a possible determinant of levels of cognitive ability between species. Recently, Charrier and colleagues reported that, in the human brain, the function of RacGAP SRGAP2 is inhibited by SRGAP2C, which is the human-specific paralog of SRGAP2, and that, when SRGAP2 is inhibited by gene KO or ectopic expression of SRGAP2C, the mouse brain acquires human-type spines with increased length and density (Charrier et al., 2012). The present study results demonstrate that disruption of RacGAP α2-chimaerin during development leads to longer, larger and densely packed spines (Figure 3). A higher cognitive function in these mice may support the attractive hypothesis that in human evolution, RacGAP function during dendritic spine development may be somehow suppressed, which leads to increased Rac activity, and results in the acquisition of the human-type spine morphological baseline and framework, and an increase in cognition (Figure S10). Our findings reveal that a *CHN1* polymorphism in rs1320875, which is located in the 5'-region of *CHN1*, is associated with cognitive ability in healthy humans (data not shown: Iwata et al., unpublished), and may also support the aforementioned hypothesis. Further studies are required to find out whether the rs1320875 SNP affects α2-chimaerin expression levels in the developing human brain.

Distinct roles of the α1- and α2-isoforms in the brain

α1- and α2-chimaerin show different biochemical properties and roles *in vitro*, and distinct spatiotemporal expression patterns in the mouse brain (Buttery et al., 2006; Hall et al., 2001; Lim et al., 1992; Van de Ven et al., 2005). However, our knowledge of the isoform-specific roles of α-chimaerin *in vivo* is very limited. By systematically generating and analyzing

isoform-specific KO mice of α-chimaerin, the present study showed that the α1- and α2-isoforms have distinct roles in brain function (Figures 2 and S1, and Table S1). For example, (1) locomotor activity increases in α2KO mice, but is normal in α1KO mice; (2) basal anxiety decreases in α2KO mice, but increases in α1KO mice; (3) hippocampus-dependent learning increases in α2KO mice, but is normal in α1KO mice. Furthermore, I performed *in vivo* overexpression experiments using *in utero* electroporation and showed that α-chimaerin isoforms regulate distinct neuronal morphological outputs, and that these effects are dependent on their N-terminal structures (Figure S9). The present study results provide the first *in vivo* evidence of distinct isoforms of a Rho-family GAP, encoded by a single gene, to play different roles in the mammalian nervous system. In flies, the RhoGAP18B isoforms, RhoGAP18B-RC and -RA, regulate distinct behavioral responses to ethanol (Rothenfluh et al., 2006). Thus, alternative splicing of Rho-family GAPs is a conserved mechanism between species, to generate a large number of functionally distinct regulators of Rho-GTPases, which in turn regulates diverse cellular processes and brain functions.

In conclusion, the present findings suggest that spine remodeling during development contributes to the adjustment of the baseline and framework of spine morphology (size and density) in adulthood, which underlies cognitive ability. Further studies are required to investigate whether there is a critical period for the baseline and framework adjustment, and if so, when this critical period starts and ends. More extensive studies are required to find out whether the spine morphological baseline and framework can be artificially shifted by changing the balance between positive and negative regulation of Rac activity during the critical period, and also in adulthood. These issues are particularly important considerations in taking a therapeutic approach to treating human neurodevelopmental disorders. Our global and conditional α2-chimaerin KO mice are promising experimental models for elucidating these problems.

EXPERIMENTAL PROCEDURES

Animals

All procedures of animal care and use were approved by the institutional guidelines of National Institute of Genetics (NIG) and RIKEN Brain Science Institute (BSI). Details are described in Extended Experimental Procedures.

Tamoxifen Administration

Tamoxifen (Sigma) was dissolved in corn oil (Sigma) at a concentration of 20 mg/ml. Both *SLICK-H*;*Chn1*$^{\alpha 2flox/+}$ and *SLICK-H*;*Chn1*$^{\alpha 2flox/-}$ mice (1-month-old) were treated with tamoxifen (0.25 mg/body weight gram) by oral gavage. Mice were dosed once daily for 5 consecutive days, rested for 10 days and then retreated for another set of 5 days, according to Heimer-McGinn and Young (2011). After 1 month of the last tamoxifen treatment, mice were used for either fear conditioning test or morphological analysis of dendritic spines.

Western Blot Analysis

Western blot analyses were performed as previously reported (Iwasato et al., 2007) with some modifications. In brief, mouse hippocampus was homogenized in Pro-PREP protein extraction solution (iNtROM Biotechnology, Inc.), and clarified by centrifugation. Proteins were separated by SDS-polyacrylamide gel electrophoresis and electroblotted to PVDF membranes. The membranes were stained with anti-actin monoclonal antibody (mAb)(1:10,000, mouse, MAB1501, Millipore), anti-α2-chimaerin polyclonal antibody (pAb)(1:10,000, rabbit)(Iwasato et al., 2007), anti-α1-chimaerin pAb (1:2,000, rabbit), appropriate species-specific HRP-conjugated secondary antibodies and detected using enhanced chemiluminescence (ECL Plus; GE Healthcare).

Open Field Test

A mouse was placed in the center of the open field apparatus (60 cm x 60 cm x 40 cm) equipped with a video camera, and its horizontal locomotor activity was monitored for 60 min. The center of the field was illuminated with 70 lux light. The distance traveled and the percentages of time spent in the center area were recorded using Image EP (O'Hara & Co.).

Homecage Activity Test

A system that automatically analyzes the locomotor activity of mice in their homecage was used. The system contains a homecage (32 cm x 18 cm x 14 cm) and filtered cage top. Spontaneous locomotor activity in the homecage was determined by utilizing photobeam interruptions by SCANET (Melquest) for 6 days. The distance between sensors was 0.5 cm. Mice were housed individually under 12 h light/dark cycle. Food and water were freely available to the mice throughout the experiment.

Elevated Plus Maze

The elevated plus maze consisted of two open arms (8 cm x 25 cm), two enclosed arms (8 cm x 25 cm x 15 cm) and a central platform (8 cm x 8 cm) arranged so that similar arms were positioned opposite to each other and perpendicular to the dissimilar arms. The whole apparatus was elevated 50 cm above the floor and illuminated with 200 lux light. Each mouse was placed in the central platform of the maze with its head facing one of the open arms, and exploratory behavior was video-recorded for 15 min. The total distance travelled, the number of arm entries, the percent entry into open or enclosed arm, the amount of time spent in each arm and the center were measured using Image EP (O'Hara & Co.).

Rotarod Test

Motor coordination and balance were examined on a constant-speed (20 revolutions per min) rotarod (Model 7600, UGO BASILE). Mice were given three trials per day, and the testing terminated upon their fall or until the maximum duration (5 min) reached.

Fear Conditioning Test

Fear conditioning test was conducted using a commercially available apparatus (O'Hara & Co.). In the conditioning session, the mouse was placed in a conditioning chamber (10 cm x 18 cm) in which a steel grid floor was wired to a shock generator. The chamber had opaque walls and was housed in a sound-attenuated box. After 2 min free exploration, the mouse was exposed to two tone-footshock parings (tone, 30 sec, 70 dB white noise; footshock, 2 sec, 0.75 mA, co-terminated with the tone, separated by 1.5 min interstimulus interval). One minute after the second footshock, the mouse was returned to its home cage. The cued fear memory test was conducted 24 h after conditioning by placing each mouse in a novel chamber (10 cm x 18 cm). The chamber had transparent walls and its floor converted with pulp bedding. The environmental cues outside the chamber and the light setup were altered. After 2 min free exploration, each mouse was exposed to tone (180 sec, 70 dB white noise). The contextual fear memory test was conducted 48 h after conditioning. The mouse was placed in the conditioning chamber for 5 min during which neither tone nor footshock was presented. Images were captured using a video camera and the area (in pixel) the mouse moved was measured. Only movement that lasted more than 2 sec and had less than 15 pixel changes was considered "freezing". Total freezing time was measured as an index of fear memory. Freezing Percentage = (total freezing time/ total testing time) x 100.

IntelliCage Test

The IntelliCage apparatus and software (NewBehavior AG) were described previously (Krackow et al., 2010; Voikar et al., 2010). IntelliCage test was performed as previously reported (Kobayashi et al., 2013) with some modifications. Radio frequency identification transponders (Planet ID GmbH) were implanted subcutaneously in the dorsocervical region. During all adaptation phases and tasks, mice were fed *ad libitum*. Adaptation phase was 3 weeks. During the first week, all doors were open; mice were free to access to all 4 corners which have water bottles (free adaptation). During the second week, all doors were closed but could be opened once per visit with a nose-poke for 5 sec (nose-poke adaptation). During the third week, mice were adapted to fixed drinking schedule (drinking session adaptation) with doors opening in response to nose-pokes between the hours of 21:00-24:00 only. The avoidance learning task was comprised of 4 sessions. In baseline session (Day 0), all doors were closed but could be opened once per visit with a nose-poke (similar to drinking session adaptation). In conditioning session (Day 1), each mouse was assigned a targeting corner in which nose-pokes triggered a 1 sec air puff instead of opening a door. After conditioning session, mice were subsequently moved to their home cage (Day 2). In probe session (Day 3), each mouse was returned to IntelliCage apparatus and counted number of corner visit. The "Visit Avoidance" was calculated by subtracting visit percentage to punished corner from the chance level (25%). In extinction session (Day 4-6), mice were free to access to all 4 corners and number of corner visit was counted. Extinction performance was quantified as Visit Avoidance normalized to the value at the probe trial (Day 3). In place preference task, water was available in only one (correct corner) of 4 corners during drinking session. This task was performed for 7 days and number of corner visit was counted for 3 h (21:00-24:00). Performance was quantified as the percentage of "Visit Preference" which is the percentage of visit to monitoring corner subtracted by the chance level

(25%). In reversal learning task, water was available in only opposite corner (new correct corner) during drinking session. This task was performed for 4 days and number of corner visit was counted for 3 h.

Histology

For histological analyses, mice were overdosed with an intraperitoneal injection of pentobarbital. Mice for immunohistochemistry were transcardially perfused with saline. Brains from perfused mice were dissected and postfixed in 4% paraformaldehyde (PFA) in 0.1 M phosphate buffer (PB). For slice preparation, microslicer (Dosaka ZERO 1) or cryostat (Leica CM 3050S) was used. Laminar structures and α2-chimaerin protein expression pattern in the hippocampus were examined with coronal sections (100 μm and 50 μm, respectively). For axonal labeling, anti-netrin-G1 pAb and anti-netrin-G2 pAb were used as described in Nishimura-Akiyoshi et al. (2007). For c-Fos protein detection, anti-c-Fos pAb (Ab-5, Calbiochem, 1:20,000) was used as described in Kobayashi et al. (2013). For α2-chimaerin protein detection, anti-α2-chimaerin pAb (1:4,000) was used as described in Iwasato et al. (2007).

Golgi-cox Staining and analysis of dendrites

Golgi-cox staining was done as described previously (Iwasato et al., 2008). Serial coronal sections (100 μm) were cuts using a microslicer (Dosaka ZERO 1). Hippocampal CA1 pyramidal neurons whose cell bodies were located at the midlevels of each section and whose dendrites were isolated from those of neighboring neurons were randomly selected from dorsal region of hippocampus under a light microscope at 20x. Images of adjacent focal planes were stacked and analyzed using ImageJ. Dendrite length and number were analyzed after importing

stacked images into IMARIS Filament Tracer software (Bitplane) and tracing neurons. Dendrite branching was studies by Scholl analysis. In brief, a series of 20 μm spaced concentric rings are brought over the soma center and Scholl measurements were obtained by quantifying the number crossing dendrites each 20 μm ring from the soma.

DiI Labeling

Mice were anesthetized with tribromoethanol (125 mg/kg, i.p.). Animals were perfused transcardially with 0.9% NaCl and 4% PFA in 0.1 M PB. Brains were trimmed and cut into a coronal section at 150 μm thickness on a microslicer (Dosaka). Lipophilic dye (DiI, Molecular Probes) was coated onto tungsten, according to Gan et al. (2000) and Mataga et al. (2004). DiI-coated particles were delivered to the slices using Helios Gene Fun (Bio-rad) system. A polycarbonate filter with a 3.0 μm pore size (BD) was inserted between the gun and the preparation. The DiI was allowed to transport for 24 h in fixative before imaging. Each slice was mounted on coverslips in VECTORSHIELD mounting media (Vector Laboratories) containing DAPI (4',6'-diamidino-2-phenylindole) for nuclear staining. In Figures S6, 3B(b), 3B(c) and 3B(d), I labeled neurons from P22-P23, P63-81, P64-P92 and P84-P89 mice, respectively.

In Utero Electroporation

In utero electroporation was performed as previously described (Mizuno et al., 2007) with some modifications. In brief, pregnant mice at E15 were anesthetized with sodium pentobarbital (50 mg/kg, i.p.) in saline. A midline laparotomy was performed to expose the uterus. For DNA microinjection, glass capillary tubes (Harvard Apparatus) were pulled using a micropipette puller (Narishige). A total of 0.5 μl of DNA solution was injected into the lateral ventricle of embryos,

and square electric pulses (40 V; 50 msec) were delivered 5 times at 1 Hz by an electroporator (NepaGene). After electroporation, the uterus was repositioned and the abdominal wall and skin were sutured.

DNA construct

The wild-type (WT) α1-chimaerin, α2-chimaerin and isoform-common-C-terminal (α1α2C) cDNAs *w*ere described previously (Iwasato et al., 2007). The GAP-inactive mutant α1-chimaerin(R304G), α2-chimaerin(R304G) and α1α2C(R304G) cDNAs were generated by a PCR-based method using primer sets: 5'-GACTCTACGGAGTGTCAGGATTTAGTG-3' / 5'-GACACTCCGTAGAGTCCTTCAGAATT-3'. These α-chimaerin cDNAs were inserted into a loxP-STOP-loxP sequence inserted pCAGplay vector (Kawaguchi and Hirano, 2006; Niwa et al., 1991), with a TagRFP (Evrogen) on the C-terminus. All coding sequences in each construct were verified by nucleotide sequencing.

Overexpression Experiment

For overexpression experiment, Cre/loxP-based supernova vector sets (H.Mi, W.Luo and T.I. unpublished: pCAG-loxP-STOP-loxP-TurboRFP-ires-tTA-WPRE [1 μg/μl] and pTRE-nlsCre [20 ng/μl]) with either one of α-chimaerin vectors (1 μg/μl) were introduced by *in utero* electroporation into the hippocampal pyramidal neurons of progeny of B6 males and ICR females: As α-chimaerin vectors I used pCAG-loxP-STOP-loxP-α1-chimaerin(WT)TagRFP, pCAG-loxP-STOP-loxP-α1-chimaerin(R304G)TagRFP, pCAG-loxP-STOP-loxP-α2-chimaerin(WT)TagRFP, pCAG-loxP-STOP-loxP-α2-chimaerin(R304G)TagRFP, pCAG-loxP-STOP-loxP-α1α2C (WT)TagRFP or pCAG-loxP-STOP-loxP-α1α2C (R304G)TagRFP. For histological analysis,

juvenile mice (P22-P23) were anesthetized with tribromoethanol (125 mg/kg, i.p.) and perfused transcardially with 0.9% NaCl and 4% PFA in 0.1 M PB. Brains were trimmed and cut into a coronal section at 150 μm thickness on a microslicer (Dosaka). Each slice was mounted on a glass slide and covered with VECTORSHIELD mounting media (Vector Laboratories) containing DAPI for nuclear staining.

In Utero Electroporation-based Neuronal Labeling

For sparse neuronal labeling of DT-α2KO and their littermate control mice, Flp/FRT-based supernova vector sets (pCAG-FRT-STOP-FRT-TurboRFP-ires-tTA-WPRE [1 μg/μl] and pTRE-nlsFlp-WPRE [50 ng/μl]) were introduced by *in utero* electroporation into the hippocampal pyramidal neurons of progeny of $Emx1^{Cre/+}$;$Chn1^{\Delta\alpha2/\Delta\alpha2}$ males and $Chn1^{\alpha2flox/\alpha2flox}$ females. Mice were anesthetized with tribromoethanol (125 mg/kg, i.p.). Animals were perfused transcardially with 0.9% NaCl and 4% PFA in 0.1 M PB. Brains were trimmed and cut into a coronal section at 150 μm thickness on a microslicer (Dosaka). Each slice was mounted on a glass slide and covered with VECTORSHIELD mounting media (Vector Laboratories) containing DAPI for nuclear staining.

Image Analysis and Quantification of Dendritic Spines

Image of dendritic spines in primary apical (Figure 3), basal (Figure S6) or oblique (Figure 4) dendrites of pyramidal neurons in CA1 region of hippocampus were taken on a Leica TSC-SP5 confocal microscopy. Sequential z-images consisted of optical sections (1024 x 1024 pixels) with 0.1 μm intervals using 63x oil immersion objective (1.3 NA) with 9x zoom. The z-images were 3D reconstructed and measured some parameters (spine length, spine maximum width, spine mean width, spine minimum width, spine area, spine volume and density) by IMARIS

Filament Tracer software (Bitplane).

Extracellular Field Potential Recording

Hippocampal slice preparation: I used 3-month-old male DT-α2KO and their littermate control mice. Animals were anesthetized with isoflurane, and the brain was quickly removed after decapitation and placed into ice-cold cutting medium (sucrose 200 mM, KCl 4.0 mM, NaH_2PO_4 1.0 mM, $NaHCO_3$ 26 mM, $MgSO_4$ 10 mM, $CaCl_2$ 0.2 mM and glucose 10 mM; bubbled with 95% CO_2 and 5% O_2). Transverse hippocampal slices (350 μm thickness) were prepared from both hemispheres using a LinearSlicer Pro7 (Dosaka). The slices were incubated in the recording medium (NaCl 119 mM, KCl 2.5 mM, NaH_2PO_4 1.0 mM, $NaHCO_3$ 26.2 mM, $MgSO_4$ 1.3 mM, $CaCl_2$ 2.5 mM and glucose 11 mM; bubbled with 95% CO_2 and 5% O_2) at 30 ˚C for at least 2 h before recording.

Extracellular recording: Shaffer collaterals were stimulated at 0.05 Hz by delivering biphasic current pulses (10-60 μA, 0.2 msec duration). Multi-planar microelectrodes arranged in 8x8 pattern with 150 μm spacing, was used for synaptic stimulation and field recording. Evoked field responses from the stratum radiatum in the CA1 area were, through 0.1-10 kHz bandpass filter, recorded at a 20 kHz sampling rate and stored for off-line analysis. Data were acquired and analyzed with MED64 Mobius software (Alpha Med Scientific Inc.). Slope of excitatory postsynaptic potential (fEPSP) and amplitude of presynaptic fiber volley (FV) were used for the comparison between genotypes.

Spine Retraction Assay

Spine retraction assay was performed as previously reported (Fu et al., 2007) with some modifications. For neuronal labeling, Cre/loxP-based supernova vector sets

(pCAG-loxP-STOP-loxP-TurboRFP-ires-tTA-WPRE [1 μg/μl] and pTRE-nlsCre [20 ng/μl]) were introduced by *in utero* electroporation into the hippocampal pyramidal neurons of progeny of $Chn1^{\Delta\alpha2/\Delta\alpha2}$ males and $Chn1^{\Delta\alpha2/+}$ females. Organotypic hippocampal slice cultures were performed using the P5 pups, according to De Simoni & Yu (2006). Retraction assay was performed on the sixth day *in vitro*. For Fc clustering, EphrinA3-Fc (R&D Systems) and Fc fragment (Jackson Immunoresearch Labs) were pre-clustered with anti-human Fc pAb (Jackson Immunoresearch Labs) in ratio of 1:4.5 and incubated at room temperature for 1 h before use. The final concentration for ephrinA3-Fc or Fc was 10 μg/ml. Each slice was treated with either pre-clustered ephrinA3-Fc or Fc for 16 h. After stimulation, slices were fixed with 4% PFA in 0.1 M PB for 30 min, and spine density of RFP-expression CA1 pyramidal neurons was visualized by confocal microscopy (Leica).

Statistical Analysis

In animal study, statistical analyses were performed using PASW Statistics version 18 or IBM SPSS Statistics version 19. To decide statistical method, the normal distribution of data was analyzed using the one-sample Kolmogorov-Smirnov test. Significance of differences was assessed as follows. For parametrical statistics, two-tailed unpaired Student's *t*-test for two independent samples or analysis of variance (ANOVA) for multiple independent samples was used. The Tukey-Kramer post hoc test was used after ANOVA indicated a significant difference. For non-parametrical statics, Mann-Whitney U-test for two independent samples or Kruskal-Wallis H test for multiple independent samples were used. $P<0.05$ was considered significant. Values are given as mean ± SEM. Asterisks in figures indicate as follows: * for $p < 0.05$, ** for $p < 0.01$, *** for $p < 0.001$

ACKNOWLEDGMENTS

This work would not have been possible without support of the help of many people. First of all, I would like to thank my supervisor, Dr. Takuji Iwasato. He gave me the opportunity for studying neuroscience, and provided me with invaluable advice on this project. I also appreciate my Progress Committee Members, Dr. Tsuyoshi Koide, Dr. Koichi Kawakami, Dr. Hiromi Hirata, Dr. Tatsumi Hirata and previous member, Dr. Yasushi Hiromi for providing me with many valuable suggestions and comments. I would like to thank Dr. Hidenobu Mizuno (NIG) for technical advice on in utero electroporation experiments, and Dr. Hiromichi Goto (RIKEN), Dr. Yuki Kobayashi (RIKEN) and Dr. Shigeyoshi Itohara (RIKEN) for technical advice on behavioral experiments, and Dr. Nobuko Mataga (RIKEN) for technical advice on the use of genegun, and Mr. Hiroshi Matsukawa (RIKEN) for help of electrophysiological experiments. I would like to thank Dr. Guoping Feng for providing SLICK-H transgenic mice. I would also like to express my gratitude to everyone in Iwasato lab. and Itohara lab. (RIKEN) for helpful discussion and advice on this project. Finally, I would like to thank my family and my former laboratory colleagues for their advice and support.

REFERENCES

Bagni, C., and Greenough, W.T. (2005). From mRNP trafficking to spine dysmorphogenesis: the roots of fragile X syndrome. Nature reviews Neuroscience *6*, 376-387.

Beck, C.H., and Fibiger, H.C. (1995). Conditioned fear-induced changes in behavior and in the expression of the immediate early gene c-fos: with and without diazepam pretreatment. The Journal of neuroscience : the official journal of the Society for Neuroscience *15*, 709-720.

Beg, A.A., Sommer, J.E., Martin, J.H., and Scheiffele, P. (2007). alpha2-Chimaerin is an essential EphA4 effector in the assembly of neuronal locomotor circuits. Neuron *55*, 768-778.

Benavides-Piccione, R., Ballesteros-Yanez, I., DeFelipe, J., and Yuste, R. (2002). Cortical area and species differences in dendritic spine morphology. Journal of neurocytology *31*, 337-346.

Bourne, J.N., and Harris, K.M. (2008). Balancing structure and function at hippocampal dendritic spines. Annual review of neuroscience *31*, 47-67.

Buttery, P., Beg, A.A., Chih, B., Broder, A., Mason, C.A., and Scheiffele, P. (2006). The diacylglycerol-binding protein alpha1-chimaerin regulates dendritic morphology. Proceedings of the National Academy of Sciences of the United States of America *103*, 1924-1929.

Cahill, M.E., Xie, Z., Day, M., Photowala, H., Barbolina, M.V., Miller, C.A., Weiss, C., Radulovic, J., Sweatt, J.D., Disterhoft, J.F.*, et al.* (2009). Kalirin regulates cortical spine morphogenesis and disease-related behavioral phenotypes. Proceedings of the National Academy of Sciences of the United States of America *106*, 13058-13063.

Canagarajah, B., Leskow, F.C., Ho, J.Y., Mischak, H., Saidi, L.F., Kazanietz, M.G., and Hurley, J.H. (2004). Structural mechanism for lipid activation of the Rac-specific GAP, beta2-chimaerin. Cell *119*, 407-418.

Carmona, M.A., Murai, K.K., Wang, L., Roberts, A.J., and Pasquale, E.B. (2009). Glial ephrin-A3 regulates hippocampal dendritic spine morphology and glutamate transport. Proceedings of the National Academy of Sciences of the United States of America *106*, 12524-12529.

Charrier, C., Joshi, K., Coutinho-Budd, J., Kim, J.E., Lambert, N., de Marchena, J., Jin, W.L., Vanderhaeghen, P., Ghosh, A., Sassa, T.*, et al.* (2012). Inhibition of SRGAP2 function by its human-specific paralogs induces neoteny during spine maturation. Cell *149*, 923-935.

Clement, J.P., Aceti, M., Creson, T.K., Ozkan, E.D., Shi, Y., Reish, N.J., Almonte, A.G., Miller, B.H., Wiltgen, B.J., Miller, C.A.*, et al.* (2012). Pathogenic SYNGAP1 mutations impair cognitive development by disrupting maturation of dendritic spine synapses. Cell *151*, 709-723.

Colon-Gonzalez, F., Leskow, F.C., and Kazanietz, M.G. (2008). Identification of an autoinhibitory mechanism that restricts C1 domain-mediated activation of the Rac-GAP alpha2-chimaerin. The Journal of biological chemistry *283*, 35247-35257.

De Simoni, A., and Yu, L.M. (2006). Preparation of organotypic hippocampal slice cultures: interface method. Nature protocols *1*, 1439-1445.

Diekmann, D., Brill, S., Garrett, M.D., Totty, N., Hsuan, J., Monfries, C., Hall, C., Lim, L., and Hall, A. (1991). Bcr encodes a GTPase-activating protein for p21rac. Nature *351*, 400-402.

Dong, J.M., Smith, P., Hall, C., and Lim, L. (1995). Promoter region of the transcriptional unit for human alpha 1-chimaerin, a neuron-specific GTPase-activating protein for p21rac. European journal of biochemistry / FEBS *227*, 636-646.

Ethell, I.M., and Pasquale, E.B. (2005). Molecular mechanisms of dendritic spine development and remodeling. Progress in neurobiology *75*, 161-205.

Fu, W.Y., Chen, Y., Sahin, M., Zhao, X.S., Shi, L., Bikoff, J.B., Lai, K.O., Yung, W.H., Fu, A.K., Greenberg, M.E.*, et al.* (2007). Cdk5 regulates EphA4-mediated dendritic spine retraction through an ephexin1-dependent mechanism. Nature neuroscience *10*, 67-76.

Gan, W.B., Grutzendler, J., Wong, W.T., Wong, R.O., and Lichtman, J.W. (2000). Multicolor "DiOlistic" labeling of the nervous system using lipophilic dye combinations. Neuron *27*, 219-225.

Hall, C., Michael, G.J., Cann, N., Ferrari, G., Teo, M., Jacobs, T., Monfries, C., and Lim, L. (2001). alpha2-chimaerin, a Cdc42/Rac1 regulator, is selectively expressed in the rat embryonic nervous system and is involved in neuritogenesis in N1E-115 neuroblastoma cells. The Journal of neuroscience : the official journal of the Society for Neuroscience *21*, 5191-5202.

Hall, C., Monfries, C., Smith, P., Lim, H.H., Kozma, R., Ahmed, S., Vanniasingham, V., Leung, T., and Lim, L. (1990). Novel human brain cDNA encoding a 34,000 Mr protein n-chimaerin, related to both the regulatory domain of protein kinase C and BCR, the product of the breakpoint cluster region gene. J Mol Biol *211*, 11-16.

Hall, C., Sin, W.C., Teo, M., Michael, G.J., Smith, P., Dong, J.M., Lim, H.H., Manser, E., Spurr, N.K., Jones, T.A.*, et al.* (1993). Alpha 2-chimerin, an SH2-containing GTPase-activating protein for the ras-related protein p21rac derived by alternate splicing of the human n-chimerin gene, is selectively expressed in brain regions and testes. Molecular and cellular biology *13*, 4986-4998.

Heimer-McGinn, V., and Young, P. (2011). Efficient inducible Pan-neuronal cre-mediated recombination in SLICK-H transgenic mice. Genesis *49*, 942-949.

Holtmaat, A., and Svoboda, K. (2009). Experience-dependent structural synaptic plasticity in the mammalian brain. Nature reviews Neuroscience *10*, 647-658.

Ip, J.P., Shi, L., Chen, Y., Itoh, Y., Fu, W.Y., Betz, A., Yung, W.H., Gotoh, Y., Fu, A.K., and Ip, N.Y. (2012). alpha2-chimaerin controls neuronal migration and functioning of the cerebral cortex through CRMP-2. Nature neuroscience *15*, 39-47.

Iwasato, T., Datwani, A., Wolf, A.M., Nishiyama, H., Taguchi, Y., Tonegawa, S., Knopfel, T., Erzurumlu, R.S., and Itohara, S. (2000). Cortex-restricted disruption of NMDAR1 impairs neuronal patterns in the barrel cortex. Nature *406*, 726-731.

Iwasato, T., Inan, M., Kanki, H., Erzurumlu, R.S., Itohara, S., and Crair, M.C. (2008). Cortical adenylyl cyclase 1 is required for thalamocortical synapse maturation and aspects of layer IV barrel development. The Journal of neuroscience : the official journal of the Society for Neuroscience *28*, 5931-5943.

Iwasato, T., Katoh, H., Nishimaru, H., Ishikawa, Y., Inoue, H., Saito, Y.M., Ando, R., Iwama, M., Takahashi, R., Negishi, M.*, et al.* (2007). Rac-GAP alpha-chimerin regulates motor-circuit formation as a key mediator of EphrinB3/EphA4 forward signaling. Cell *130*, 742-753.

Kanki, H., Suzuki, H., and Itohara, S. (2006). High-efficiency CAG-FLPe deleter mice in C57BL/6J background. Experimental animals / Japanese Association for Laboratory Animal Science *55*, 137-141.

Kasai, H., Fukuda, M., Watanabe, S., Hayashi-Takagi, A., and Noguchi, J. (2010). Structural dynamics of dendritic spines in memory and cognition. Trends Neurosci *33*, 121-129.

Kawaguchi, S.Y., and Hirano, T. (2006). Integrin alpha3beta1 suppresses long-term potentiation at inhibitory synapses on the cerebellar Purkinje neuron. Molecular and cellular neurosciences *31*, 416-426.

Kawase, E., Suemori, H., Takahashi, N., Okazaki, K., Hashimoto, K., and Nakatsuji, N. (1994). Strain difference in establishment of mouse embryonic stem (ES) cell lines. The International journal of developmental biology *38*, 385-390.

Kim, J.J., and Fanselow, M.S. (1992). Modality-specific retrograde amnesia of fear. Science *256*, 675-677.

Klein, R. (2009). Bidirectional modulation of synaptic functions by Eph/ephrin signaling. Nature neuroscience *12*, 15-20.

Kobayashi, Y., Sano, Y., Vannoni, E., Goto, H., Suzuki, H., Oba, A., Kawasaki, H., Kanba, S., Lipp, H.P., Murphy, N.P.*, et al.* (2013). Genetic dissection of medial habenula-interpeduncular nucleus pathway function in mice. Frontiers in behavioral neuroscience *7*, 17.

Krackow, S., Vannoni, E., Codita, A., Mohammed, A.H., Cirulli, F., Branchi, I., Alleva, E., Reichelt, A., Willuweit, A., Voikar, V.*, et al.* (2010). Consistent behavioral phenotype differences between inbred mouse strains in the IntelliCage. Genes, brain, and behavior *9*, 722-731.

LeDoux, J.E. (2000). Emotion circuits in the brain. Annual review of neuroscience *23*, 155-184.

Lim, H.H., Michael, G.J., Smith, P., Lim, L., and Hall, C. (1992). Developmental regulation and neuronal expression of the mRNA of rat n-chimaerin, a p21rac GAP:cDNA sequence. The Biochemical journal *287 (Pt 2)*, 415-422.

Ma, X.M., Kiraly, D.D., Gaier, E.D., Wang, Y., Kim, E.J., Levine, E.S., Eipper, B.A., and Mains, R.E. (2008). Kalirin-7 is required for synaptic structure and function. The Journal of neuroscience : the official journal of the Society for Neuroscience *28*, 12368-12382.

Mataga, N., Mizuguchi, Y., and Hensch, T.K. (2004). Experience-dependent pruning of dendritic spines in visual cortex by tissue plasminogen activator. Neuron *44*, 1031-1041.

Miyake, N., Chilton, J., Psatha, M., Cheng, L., Andrews, C., Chan, W.M., Law, K., Crosier, M., Lindsay, S., Cheung, M.*, et al.* (2008). Human CHN1 mutations hyperactivate alpha2-chimaerin and cause Duane's retraction syndrome. Science *321*, 839-843.

Mizuno, H., Hirano, T., and Tagawa, Y. (2007). Evidence for activity-dependent cortical wiring: formation of interhemispheric connections in neonatal mouse visual cortex requires projection neuron activity. The Journal of neuroscience : the official journal of the Society for Neuroscience *27*, 6760-6770.

Murai, K.K., Nguyen, L.N., Irie, F., Yamaguchi, Y., and Pasquale, E.B. (2003). Control of hippocampal dendritic spine morphology through ephrin-A3/EphA4 signaling. Nature neuroscience *6*, 153-160.

Nimchinsky, E.A., Oberlander, A.M., and Svoboda, K. (2001). Abnormal development of dendritic spines in FMR1 knock-out mice. The Journal of neuroscience : the official journal of the Society for Neuroscience *21*, 5139-5146.

Nimchinsky, E.A., Sabatini, B.L., and Svoboda, K. (2002). Structure and function of dendritic spines. Annual review of physiology *64*, 313-353.

Nishimura-Akiyoshi, S., Niimi, K., Nakashiba, T., and Itohara, S. (2007). Axonal netrin-Gs transneuronally determine lamina-specific subdendritic segments. Proceedings of the National Academy of Sciences of the United States of America *104*, 14801-14806.

Niwa, H., Yamamura, K., and Miyazaki, J. (1991). Efficient selection for high-expression transfectants with a novel eukaryotic vector. Gene *108*, 193-199.

Penzes, P., Cahill, M.E., Jones, K.A., VanLeeuwen, J.E., and Woolfrey, K.M. (2011). Dendritic spine pathology in neuropsychiatric disorders. Nature neuroscience *14*, 285-293.

Phillips, R.G., and LeDoux, J.E. (1992). Differential contribution of amygdala and hippocampus to cued and contextual fear conditioning. Behavioral neuroscience *106*, 274-285.

Rothenfluh, A., Threlkeld, R.J., Bainton, R.J., Tsai, L.T., Lasek, A.W., and Heberlein, U. (2006). Distinct behavioral responses to ethanol are regulated by alternate RhoGAP18B isoforms. Cell *127*, 199-211.

Shi, L., Fu, W.Y., Hung, K.W., Porchetta, C., Hall, C., Fu, A.K., and Ip, N.Y. (2007). Alpha2-chimaerin interacts with EphA4 and regulates EphA4-dependent growth cone collapse. Proceedings of the National Academy of Sciences of the United States of America *104*, 16347-16352.

Van de Ven, T.J., VanDongen, H.M., and VanDongen, A.M. (2005). The nonkinase phorbol ester receptor alpha 1-chimerin binds the NMDA receptor NR2A subunit and regulates dendritic spine density. The Journal of neuroscience : the official journal of the Society for Neuroscience *25*, 9488-9496.

Voikar, V., Colacicco, G., Gruber, O., Vannoni, E., Lipp, H.P., and Wolfer, D.P. (2010). Conditioned response suppression in the IntelliCage: assessment of mouse strain differences and effects of hippocampal and striatal lesions on acquisition and retention of memory. Behavioural brain research *213*, 304-312.

Wegmeyer, H., Egea, J., Rabe, N., Gezelius, H., Filosa, A., Enjin, A., Varoqueaux, F., Deininger, K., Schnutgen, F., Brose, N.*, et al.* (2007). EphA4-dependent axon guidance is mediated by the RacGAP alpha2-chimaerin. Neuron *55*, 756-767.

Young, P., Qiu, L., Wang, D., Zhao, S., Gross, J., and Feng, G. (2008). Single-neuron labeling with inducible Cre-mediated knockout in transgenic mice. Nature neuroscience *11*, 721-728.

Yuste, R., and Bonhoeffer, T. (2001). Morphological changes in dendritic spines associated with long-term synaptic plasticity. Annual review of neuroscience *24*, 1071-1089.

Zuo, Y., Lin, A., Chang, P., and Gan, W.B. (2005). Development of long-term dendritic spine stability in diverse regions of cerebral cortex. Neuron *46*, 181-189.

FIGURE LEGENDS

Figure 1. Isoform-specific and pan-isoform α-chimaerin flox and KO mouse lines

(A) Schematics for wild-type (WT) and isoform-specific and pan-isoform flox and knockout (KO) alleles of α-chimaerin (αChn). In the α2-isoform-specific flox (α2-flox) allele, the α2-isoform-specific exon 6 is flanked by two loxP sites; this exon is deleted in the α2-specific αChnKO (α2KO) allele. In the α1-isoform-specific flox (α1-flox) allele, the α1-specific locus surrounding the transcriptional initiation site is flanked by two loxPs; this locus is deleted in the α1-specific αChnKO (α1KO) allele. In the pan-isoform flox (αChn-flox) allele, exons 9 and 10, which are common to both α1- and α2-isoforms, and code for the amino acids essential for RacGAP activity, are flanked by two loxP sites. In the αChnKO allele, exons 9 and 10 are deleted. All of these flox mice were generated by gene targeting using MS12 ES cells derived from the B6 strain, and KO mice were generated by expressing Cre recombinase in the germline of the flox mice.

(B) Western blot analyses of the P14 hippocampus using α1-chimaerin-specific and α2-chimaerin-specifc antibodies. Normal levels of α1- and α2-chimaerin (black arrowhead) were detected in the αChn-flox ($Chn1^{flox/flox}$), α2-flox ($Chn1^{\alpha 2flox/\alpha 2flox}$), and α1-flox ($Chn1^{\alpha 1flox/\alpha 1flox}$) mice; only the truncated α1- and α2-chimaerin (white arrowhead), which lack RacGAP activity (Iwasato et al., 2007), were detected in the αChnKO ($Chn1^{-/-}$) mice; α1-chimaerin, but not α2-chimaerin, was lacking in α1KO ($Chn1^{\Delta\alpha 1/\Delta\alpha 1}$) mice; α2-chimaerin, but not α1-chimaerin, was lacking in the α2KO ($Chn1^{\Delta\alpha 2/\Delta\alpha 2}$) mice.

Figure 2. Isoform-specific and time-dependent roles of α-chimaerin on learning and memory

(A) Contextual fear learning is increased in the following mice: **(a)** αChnKO (*p<0.05; Cued: p=0.34); **(b)** DT-αChnKO (**p<0.01; Cued: p=0.99); **(d)** α2KO (*p<0.05; Cued: p=0.70); **(e)** DT-α2KO (*p<0.05; Cued: p=0.64); but not in **(c)** α1KO (p=0.79; Cued: p=0.59); or **(f)** Ad-α2KO (p=0.50; Cued: p=0.40) mice.

(B) Summary of the representative phenotypes of the KO mouse lines in fear conditioning test.

(C) The "Visit Avoidance" was calculated by subtracting the visit percentage to punishment corner from the chance level (25%). **(a)** The percentage of Visit Avoidance during the baseline session and probe trial (Baseline: p=0.84, Probe: *p<0.05). **(b)** Extinction performance was quantified as the Visit Avoidance normalized to the value of the probe trial. α2KO mice showed normal extinction (two-way ANOVA; $F_{(1,19)}$=0.048, p=0.83 for genotype).

(D) In the place preference and reversal learning tests, the performance was quantified as the percentage of "Visit Preference", which is the percentage of visits to the monitoring corner subtracted by the chance level (25%). **(a)** Experimental scheme. **(b)** The Visit Preference in the place preference learning test (two-way ANOVA; $F_{(1,20)}$=3.61, p=0.07 for genotype). **(c)** The Visit Preference in the reversal learning test (two-way ANOVA; $F_{(1,20)}$=2.78, p=0.11 for genotype). Data are shown as mean±SEM.

Figure 3. α2-chimaerin regulates size and density of hippocampal dendritic spines

(A) Typical morphology of a sparsely labeled hippocampal CA1 pyramidal neuron (P24).

(B) (a) Representative images of RFP-labeled apical dendrites of hippocampal CA1 cells from DT-α2KO mice and their control mice at P24. Juvenile DT-α2KO mice showed significantly increased dendritic spine length and volume compared with the control mice (Spine length: ***p<0.001, Spine volume: ***p<0.001), but spine density was not altered between genotypes (p=0.49). **(b)** Representative images of DiI-labeled apical dendrites of hippocampal CA1 cells

from DT-α2KO mice and their control mice in adulthood. Adult DT-α2KO mice showed significantly increased dendritic spine length and volume compared with the control mice (Spine length: **p<0.01, Spine volume: p<0.05). The dendritic spine density was also increased in adult DT-α2KO mice compared with the control mice (*p<0.05). **(c)** Representative images of DiI-labeled apical dendrites of hippocampal CA1 cells from DT-α1KO mice and their control mice in adulthood. Adult DT-α1KO mice showed normal spine morphology and density. There were no significant difference between DT-α1KO mice and their control mice (Spine length: p=0.78, Spine volume: p=0.54, Spine density: p=0.54). **(d)** Representative images of DiI-labeled apical dendrites of hippocampal CA1 cells from Ad-α2KO mice and their control mice in adulthood. Ad-α2KO mice showed significantly decreased spine length and increased spine volume compared with the control mice (Spine length: ***p<0.001, Spine volume: **p<0.01). The spine density was not altered between genotypes (p=0.053). Spine length and spine volume: Mann-Whitney U-test. Scale bar, 2 μm.

(C) The dendritic spine density of adult control mice is significantly lower than that of the juvenile control mice (**p<0.01); while the spine density of the adult DT-α2KO mice did not significantly differ from that of the juvenile DT-α2KO mice (p=0.38).

Figure 4. α2-chimaerin negatively regulates spine size in a RacGAP activity-dependent and cell-autonomous manner

(A) Schematic representation of expression constructs. Each of these proteins fused to monomeric RFP in their C-terminal regions.

(B) Representative images of RFP-labeled oblique dendrites of hippocampal CA1 cells at P22-P23. Hippocampal CA1 pyramidal neurons expressing RFP alone (Control), RFP and wild-type α2-chimaerin (WT), or RFP and RacGAP deficient α2-chimaerin mutant (R304G).

WT α2-chimaerin overexpression (OE) neurons showed decreased spine length and volume compared with the control neurons ([Spine length, Kruskal-Wallis H test: ***p<0.001, Mann-Whitney U-test with a Bonferroni correction, WT: ***p<0.001, R304G: p=0.63 versus control, respectively], [Spine volume, Kruskal-Wallis H test: **p<0.01, Mann-Whitney U-test with a Bonferroni correction, WT: **p<0.01, R304G: p=1.00 versus control, respectively]). The spine density was not significant difference between WT α2-chimaerin overexpression neurons compared with the control neurons (one-way ANOVA: $F_{(2,52)}$=4.13, *p<0.05 for genotype, with Bonferroni correction, WT: p=0.25, R304G: p=0.30 versus control, respectively). Scale bar, 2 μm. Data are shown as mean±SEM.

Figure 5. Suppression of ephrinA3-induced spine retraction in the CA1 pyramidal neurons of organotypic slice cultures of the α2KO mouse hippocampus

(A) Typical morphology of a sparsely labeled RFP-expressing hippocampal pyramidal neurons in organotypic hippocampal slices (DIV6) prepared from neonatal (P5) mice. Scale bar, 100 μm.

(B) Segments of dendrites from hippocampal slices from the α2KO and control mice, after treatment with eprhinA3-Fc or Fc. Scale bar, 10 μm.

(C) The spine density was quantified after treatment with ephrinA3-Fc or Fc. The total spine density does not change with Fc treatments between genotypes (p=0.79). EphrinA3-Fc-induced spine retraction was suppressed in α2KO neurons (***p<0.001). Data are shown as mean±SEM.

Figure 6. A model for the regulation of spine morphogenesis and animal behavior by α2-chimaerin

(A) In the developing hippocampus of WT mice, ephrinA3 expressed on astrocytes activates EphA4 on the postsynaptic neuron and restricts the growth of dendritic spines (Murai et al.,

2003). The ephrinA3/EphA4 forward-signaling pathway inactivates Rac through α2-chimaerin, leading to spine retraction/elimination.

(B) In the developing hippocampus of α2KO mice, the absence of α2-chimaerin results in a loss of the ephrinA3/EphA4 forward-signaling pathway, and subsequent activation of Rac, which then accelerates the actin polymerization, leading to increased spine size and suppressed spine elimination. These spine abnormalities persisted into adulthood and contribute to increased synaptic transmission, and hippocampus-dependent learning.

FIGURE 1

A

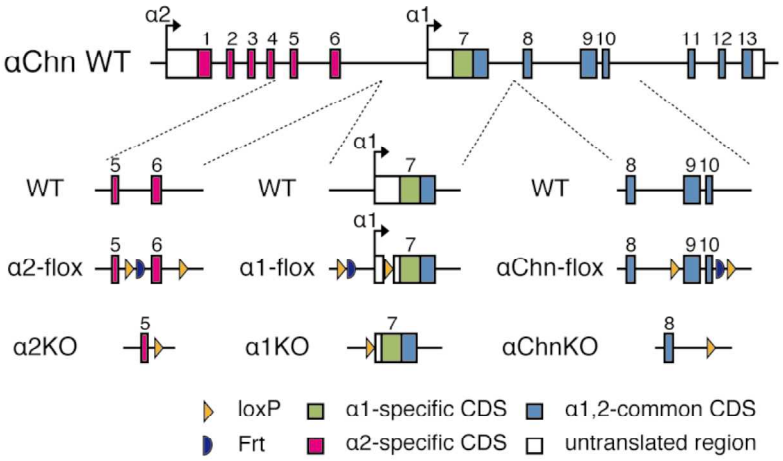
α2
α1
αChn WT
1 2 3 4 5 6 7 8 9 10 11 12 13
WT
WT
WT
α2-flox
α1-flox
αChn-flox
α2KO
α1KO
αChnKO
loxP
Frt
α1-specific CDS
α2-specific CDS
α1,2-common CDS
untranslated region

B

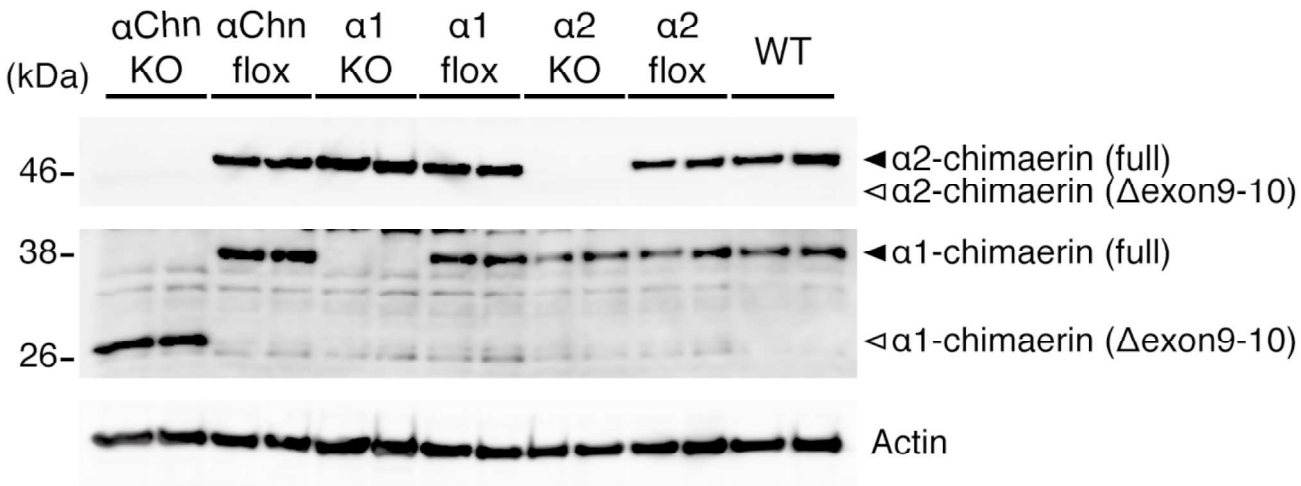
(kDa)
αChn KO
αChn flox
α1 KO
α1 flox
α2 KO
α2 flox
WT
46-
38-
26-
◄α2-chimaerin (full)
◅α2-chimaerin (Δexon9-10)
◄α1-chimaerin (full)
◅α1-chimaerin (Δexon9-10)
Actin

FIGURE 2

A Fear Learning

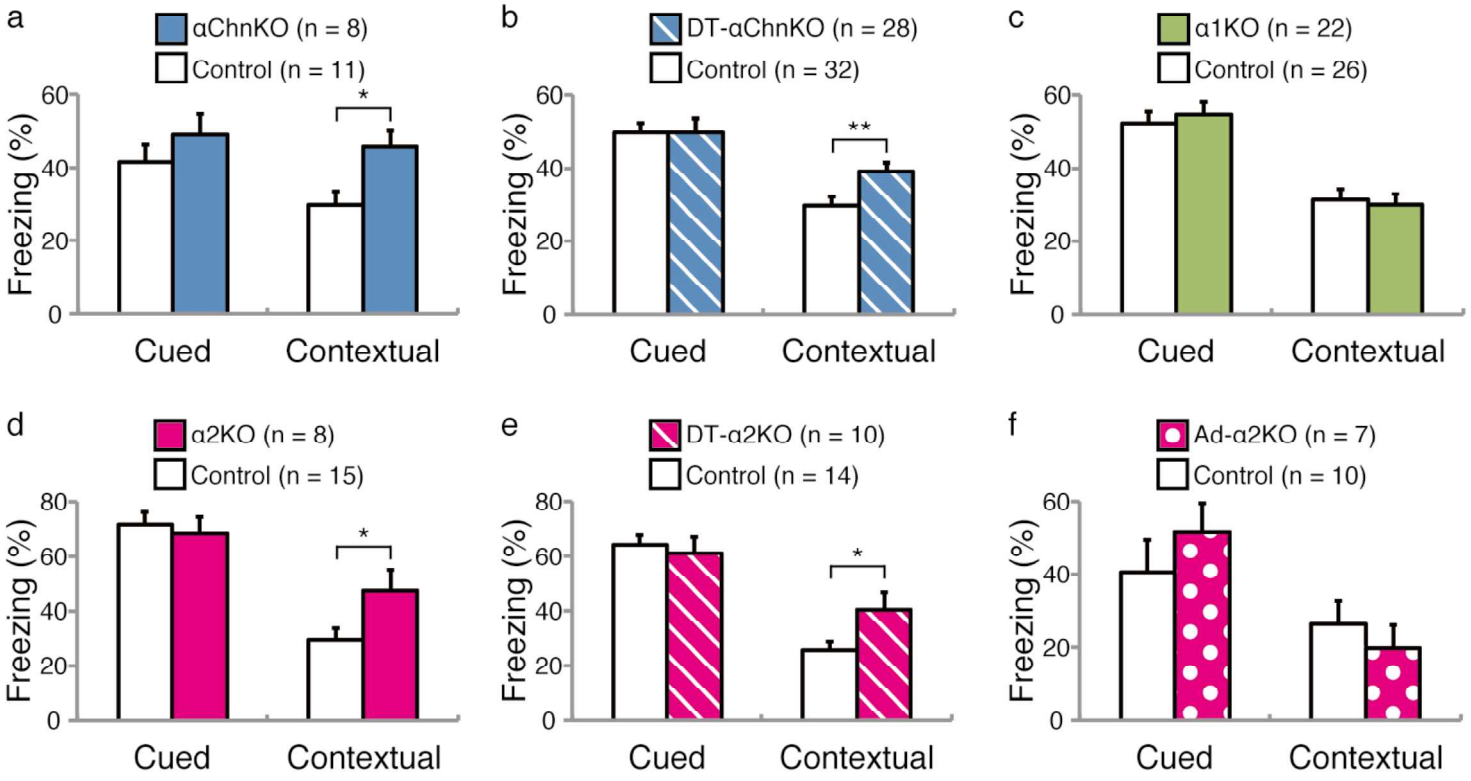

B Fear Learning

Mouse line	Disrupted isoform	Deleted pattern	Behavioral phenotypes	
			Cued fear learning	Contextual fear learning
αChnKO	α1, α2	Global	Normal	Increased
DT-αChnKO		Dorsal telencephalon-specific	Normal	Increased
α1KO	α1	Global	Normal	Normal
α2KO	α2	Global	Normal	Increaed
DT-α2KO		Dorsal telencephalon-specific	Normal	Increased
Ad-α2KO		Adult-specific	Normal	Normal

C Avoidance Learning (IntelliCage)

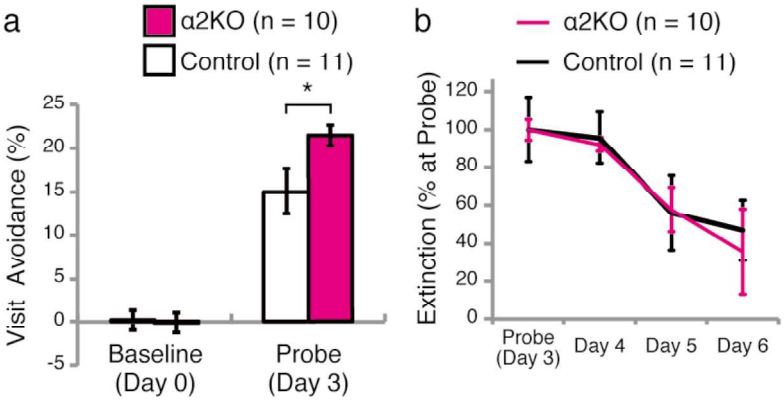

D Place Preference Learning & Reversal Learning (IntelliCage)

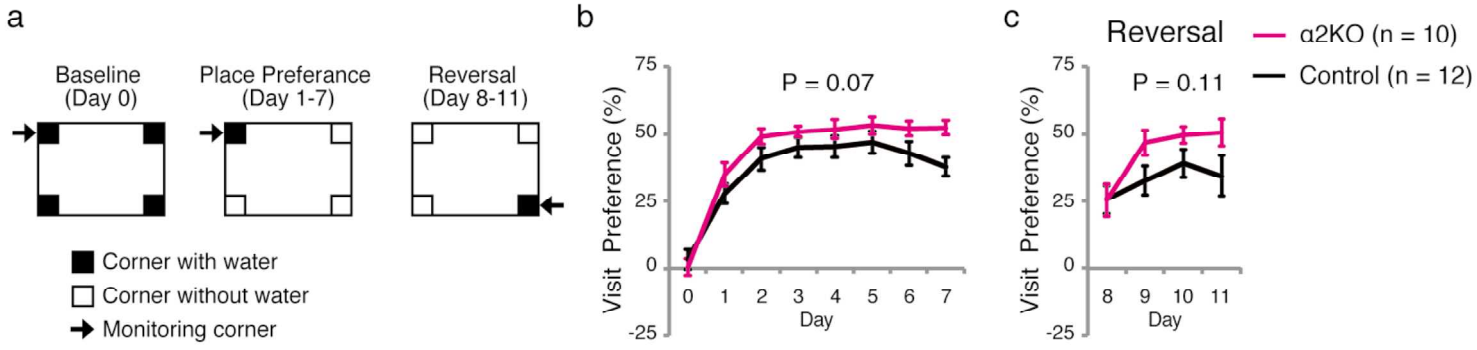

FIGURE 3

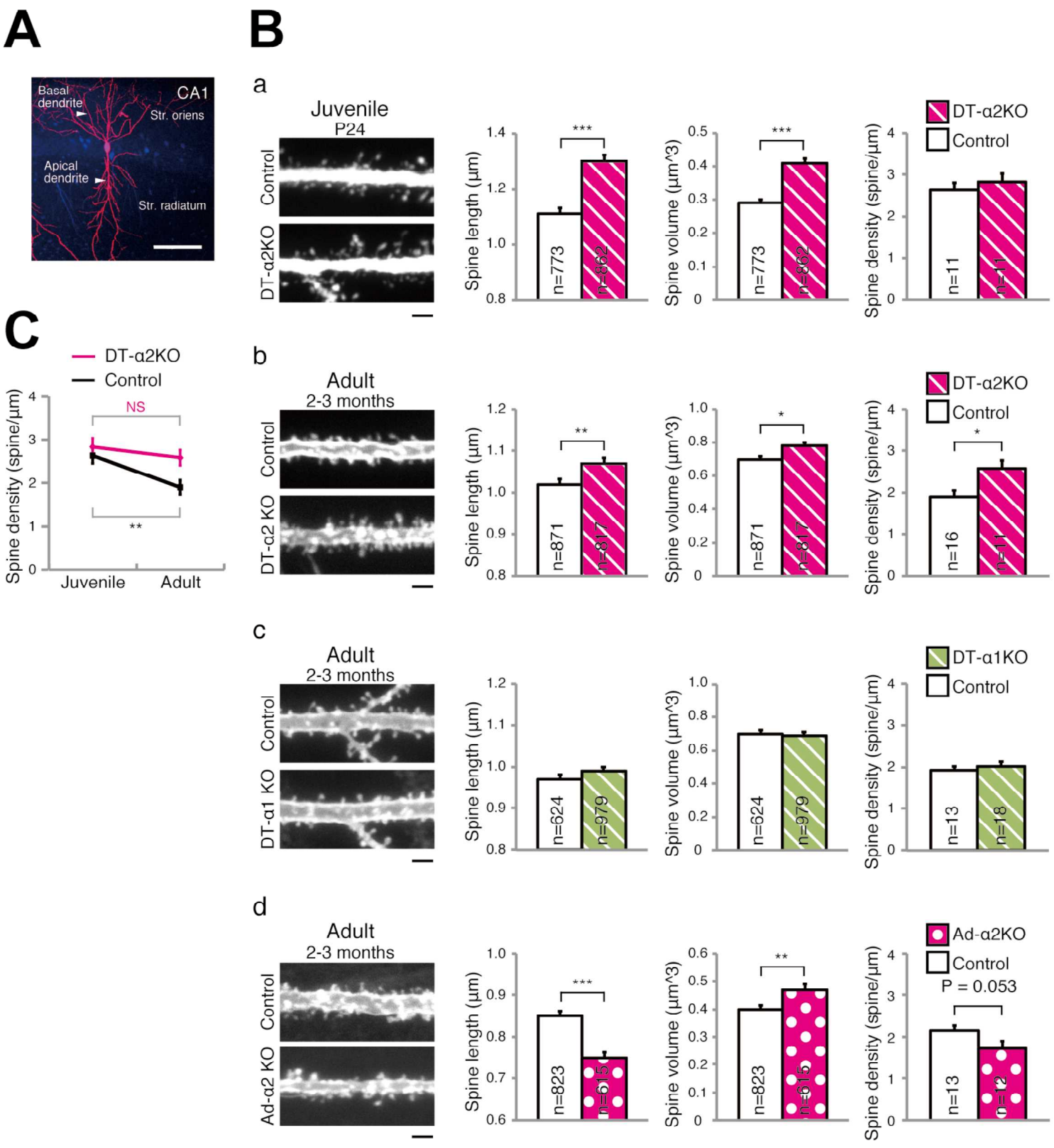
A
Basal dendrite
CA1
Str. oriens
Apical dendrite
Str. radiatum
B
a
Juvenile
P24
Control
DT-α2KO
Spine length (μm)
Spine volume (μm^3)
Spine density (spine/μm)
DT-α2KO
Control
n=773
n=862
n=11
n=11
b
Adult
2-3 months
Control
DT-α2 KO
n=871
n=817
n=16
n=11
c
Adult
2-3 months
Control
DT-α1 KO
DT-α1KO
Control
n=624
n=979
n=13
n=18
d
Adult
2-3 months
Control
Ad-α2 KO
Ad-α2KO
Control
P = 0.053
n=823
n=615
n=13
n=12
C
DT-α2KO
Control
NS
Spine density (spine/μm)
Juvenile
Adult

FIGURE 4

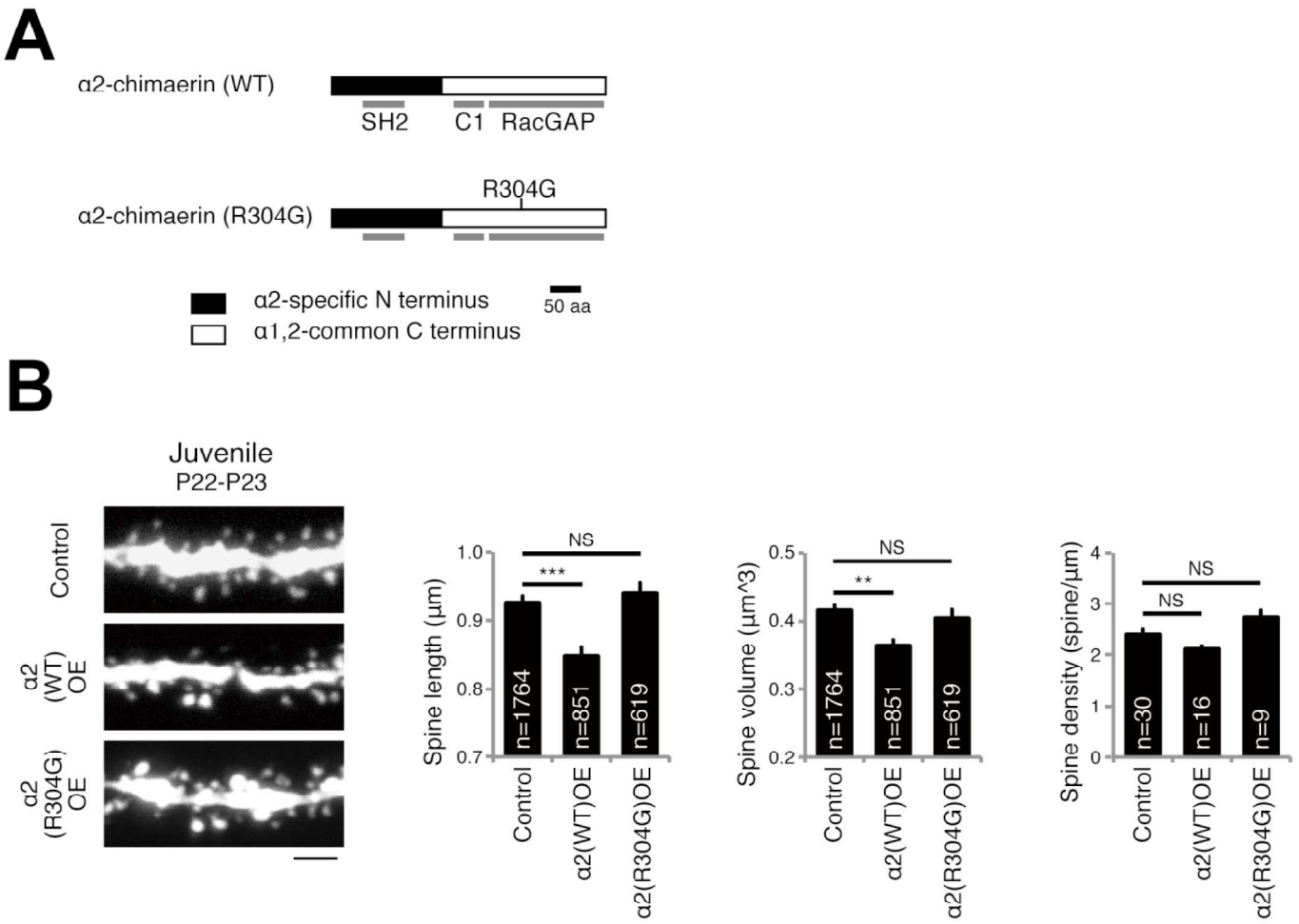
A
α2-chimaerin (WT)
SH2
C1
RacGAP
α2-chimaerin (R304G)
R304G
α2-specific N terminus
α1,2-common C terminus
50 aa
B
Juvenile
P22-P23
Control
α2 (WT) OE
α2 (R304G) OE
Spine length (μm)
Spine volume (μm^3)
Spine density (spine/μm)
NS
***
**
n=1764
n=851
n=619
n=30
n=16
n=9
Control
α2(WT)OE
α2(R304G)OE

FIGURE 5

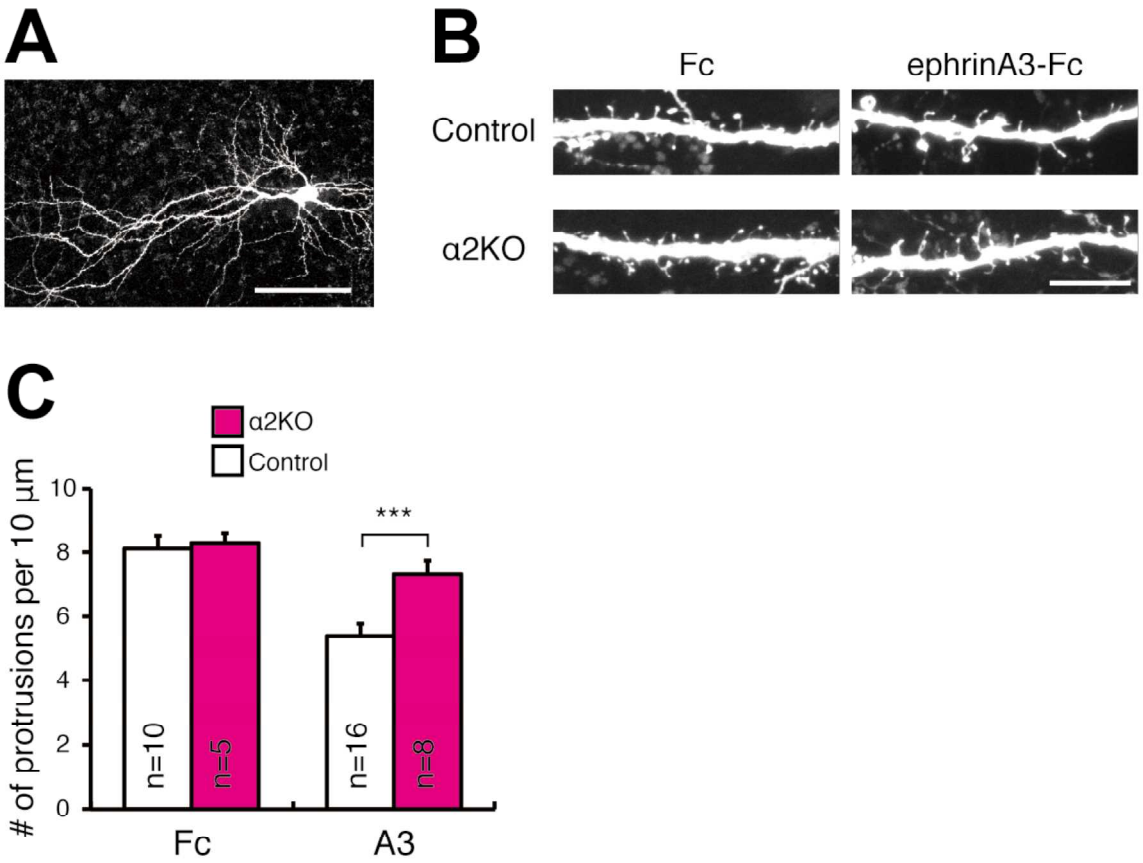
A
B
Fc
ephrinA3-Fc
Control
α2KO
C
α2KO
Control
# of protrusions per 10 µm
10
8
6
4
2
0
***
n=10
n=5
n=16
n=8
Fc
A3

FIGURE 6

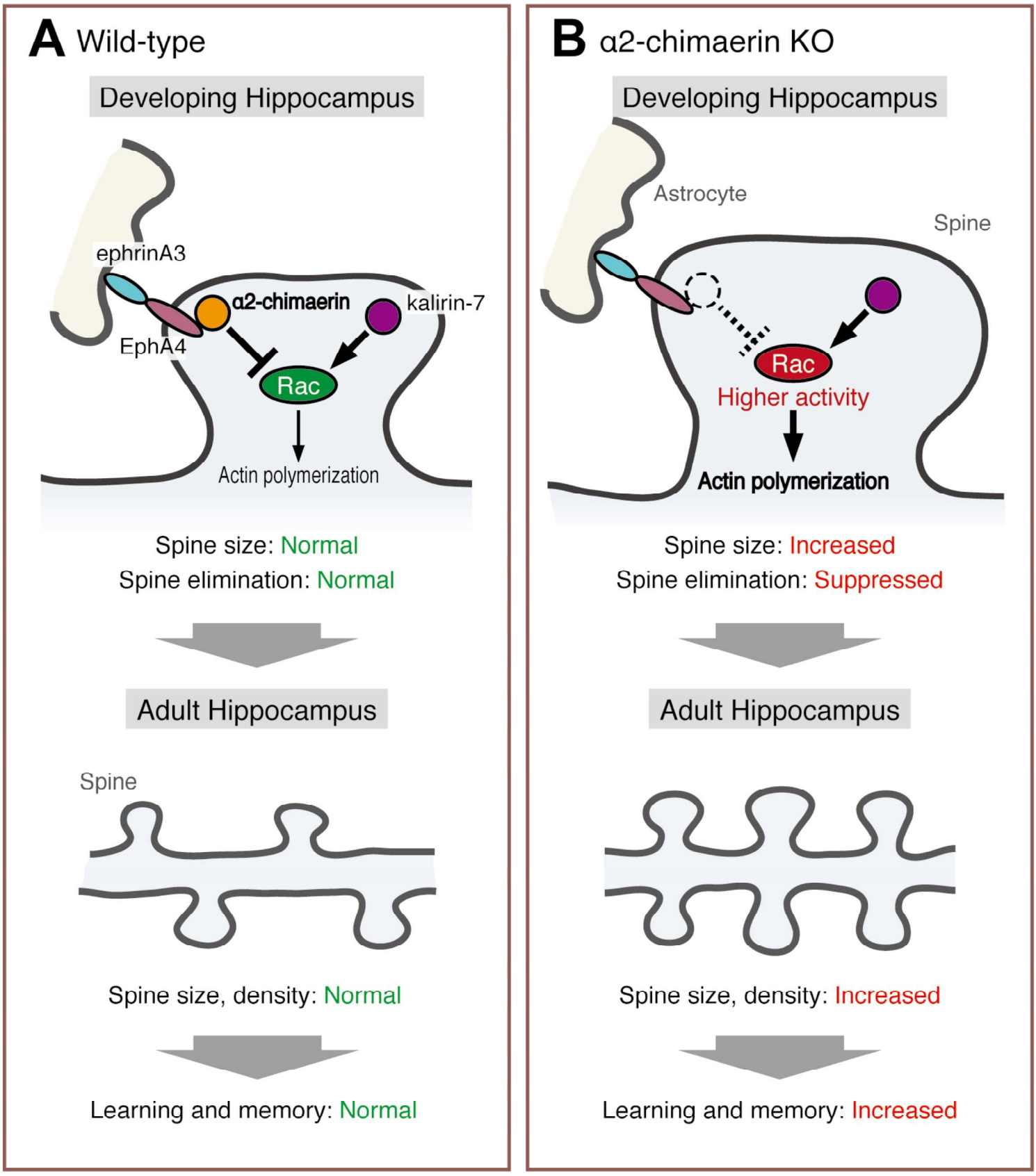
A Wild-type
Developing Hippocampus
ephrinA3
α2-chimaerin
kalirin-7
EphA4
Rac
Actin polymerization
Spine size: Normal
Spine elimination: Normal
Adult Hippocampus
Spine
Spine size, density: Normal
Learning and memory: Normal
B α2-chimaerin KO
Developing Hippocampus
Astrocyte
Spine
Rac
Higher activity
Actin polymerization
Spine size: Increased
Spine elimination: Suppressed
Adult Hippocampus
Spine size, density: Increased
Learning and memory: Increased

INVENTORY OF SUPPLEMENTAL INFORMATION

Table S1. Summary of the representative phenotypes of the KO mouse lines. Locomotor activity, motor coordination, and basal anxiety were investigated using open field, constant speed rotarod and elevated plus maze tests, respectively.

Mouse line	Disrupted isoform	Deleted pattern	Behavioral phenotypes			
			Gait	Locomotor activity	Motor coordination	Basal anxiety
αChnKO[1)]	α1, α2	Global	Hopping	Increased[2)]	Impaired	Decreased
DT-αChnKO	α1, α2	DT-specific	Normal	Normal	Normal	Normal
α1KO	α1	Global	Normal	Normal	Normal	Increased
α2KO	α2	Global	Hopping	Increased	Impaired	Decreased[3)]

[1)]=spontaneous mutant (*Chn1*$^{mfy/mfy}$) and targeted mutant (*Chn1*$^{-/-}$), [2)]=Increased locomotor activity was also detected in the homecage activity test, [3)]=Decreased basal anxiety level was also detected in the open field test.

Figure S1

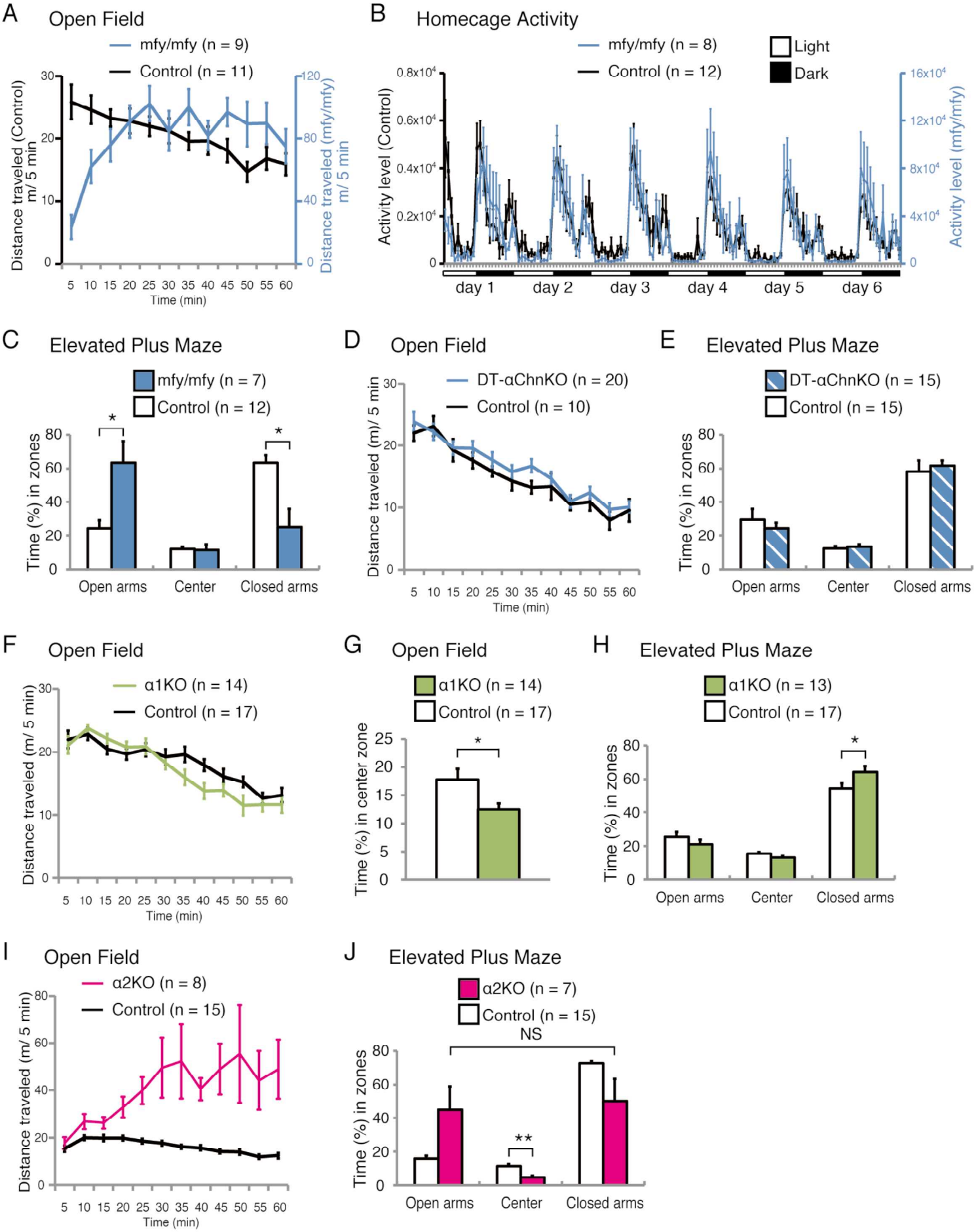
A
Open Field
mfy/mfy (n = 9)
Control (n = 11)
Distance traveled (Control) m/ 5 min
Distance traveled (mfy/mfy) m/ 5 min
Time (min)
B
Homecage Activity
mfy/mfy (n = 8)
Control (n = 12)
Light
Dark
Activity level (Control)
Activity level (mfy/mfy)
day 1
day 2
day 3
day 4
day 5
day 6
C
Elevated Plus Maze
mfy/mfy (n = 7)
Control (n = 12)
Time (%) in zones
Open arms
Center
Closed arms
D
Open Field
DT-αChnKO (n = 20)
Control (n = 10)
Distance traveled (m)/ 5 min
Time (min)
E
Elevated Plus Maze
DT-αChnKO (n = 15)
Control (n = 15)
Time (%) in zones
Open arms
Center
Closed arms
F
Open Field
α1KO (n = 14)
Control (n = 17)
Distance traveled (m/ 5 min)
Time (min)
G
Open Field
α1KO (n = 14)
Control (n = 17)
Time (%) in center zone
H
Elevated Plus Maze
α1KO (n = 13)
Control (n = 17)
Time (%) in zones
Open arms
Center
Closed arms
I
Open Field
α2KO (n = 8)
Control (n = 15)
Distance traveled (m/ 5 min)
Time (min)
J
Elevated Plus Maze
α2KO (n = 7)
Control (n = 15)
NS
Time (%) in zones
Open arms
Center
Closed arms

Figure S1. Representative behavioral phenotypes of a series of α-chimaerin mutant lines

(A) In open field test, total distance traveled of αChn-deficient mice was 4-fold greater than that of control mice (Control: 244.5±17.6 m, *mfy*/*mfy*: 973.1±93.3 m, ***p<0.001), although for the first 5 min, there was no significant difference in locomotor activity between genotypes (p>0.05)

(B) In homecage activity test, αChn-deficient mice showed extremely increased locomotor activity. The number of photobeam interruptions was significantly increased in αChn-deficient mice ([light cycle, Control: 7009.7±1935.9 cases/day, *mfy*/*mfy*: 59161.1±24896.4 cases/day, **p<0.01], [dark cycle, Control: 24214.9±5459.1 cases/day, *mfy*/*mfy*: 512331.7±202719.5 cases/day, **p<0.01 for genotype]).

(C) αChn-deficient mice exhibited decreased anxiety-like behavior. Mice fear unclosed space and avoid staying in open arms. The mice were placed on the elevated plus maze for 10 min and percent time spent in the each zone was analyzed. αChn-deficient mice exhibited a significant increase in the percentage of time spent in open arms and a decrease in the percentage of time spent in closed arms compared with control (*p<0.05).

(D) Locomotor activity was not altered in DT-αChnKO mice. There was no significant difference between genotypes in total distance traveled (Control: 177.8±10.2m, DT-αChnKO: 193.5±10.5m, p=0.35).

(E) DT-αChnKO mice showed normal anxiety-like behavior. The time spent in each zone was not different between control and DT-αChnKO mice (open: p=0.51, center: p=0.54, closed: p=0.62)

(F) Locomotor activity was not altered in α1KO mice. Total distance traveled was not different between genotypes (Control: 218.9±7.0m, α1KO: 204.9±8.2m, p=0.20).

(G-H) α1KO mice showed increased anxiety-like behavior in both open field and elevated plus maze; (G) α1KO mice displayed decreased percentage of time spent in the center position compared with their control mice in open filed (*p<0.05); (H) α1KO mice displayed increased percentage of time spent in closed arms in elevated plus maze (*p<0.05).

(I) α2KO mice displayed higher locomotor activity in open field. Total distance traveled by α2KO mice was significantly greater than that of control mice (Control: 195.1±9.0m, α2KO: 482.7±96.2m, *p<0.05).

(J) α2KO mice displayed decreased anxiety-like behavior in elevated plus maze. α2KO mice showed no preference for closed arm. The percentage of spent time is not altered between open arms and closed arms in α2KO mice (p=0.79). α2KO mice displayed decreased percentage of time spent in center position (**p<0.01). Data are shown as mean±SEM.

Figure S2

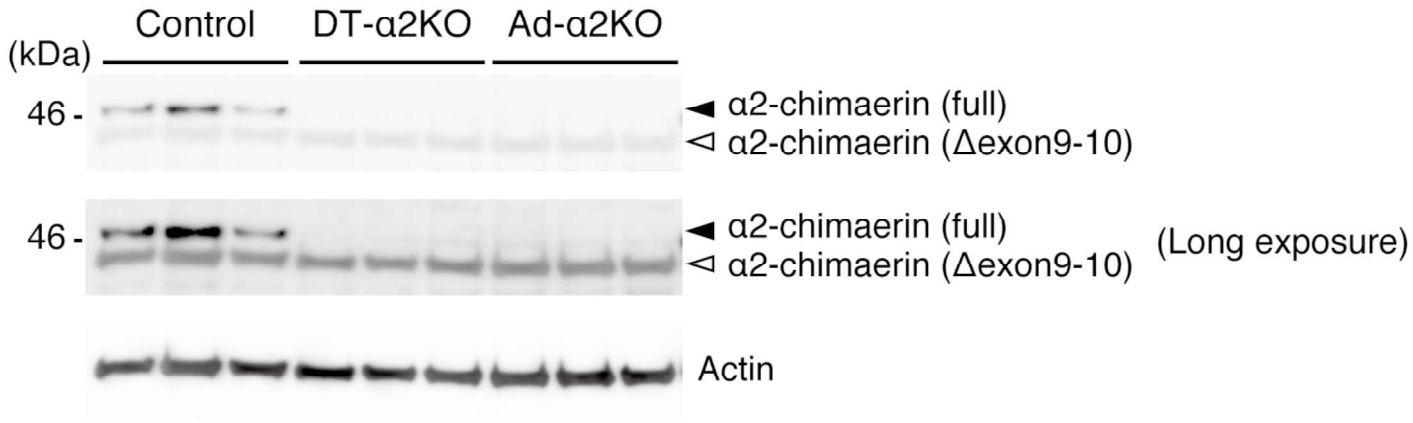
Control
DT-α2KO
Ad-α2KO
(kDa)
46 -
◄ α2-chimaerin (full)
◅ α2-chimaerin (Δexon9-10)
46 -
◄ α2-chimaerin (full)
◅ α2-chimaerin (Δexon9-10)
(Long exposure)
Actin

Figure S2. Western blot analyses of α-chimaerin mutant mouse lines

Western blot analysis of the adult (3-month-old) hippocampus using an α2-chimaerin-specific antibody for control (*Chn1*$^{\alpha 2flox/-}$), DT-α2KO (*Emx1*$^{Cre/+}$;*Chn1*$^{\alpha 2flox/-}$) and Ad-α2KO (tamoxifen-treated *SLICK-H*;*Chn1*$^{\alpha 2flox/-}$) mice. In DT-α2KO and Ad-α2KO mice, α2-chimaerin protein (full) was undetectable even with longer exposure. Black arrowheads indicate intact α2-chimaerin (full length). White arrowheads indicate truncated α2-chimaerin (Δexon 9-10), which lacks RacGAP activity and is expressed from the αChn KO allele.

Figure S3

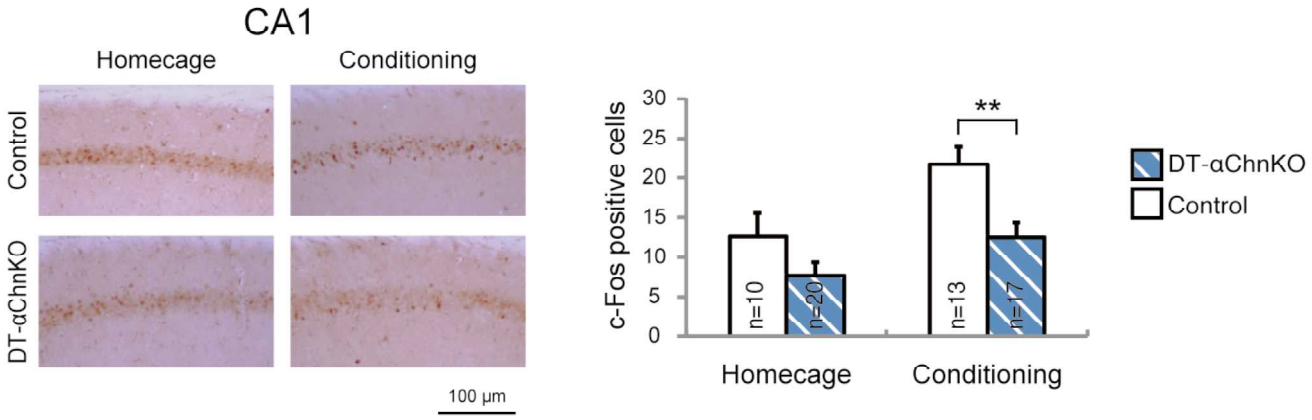
CA1
Homecage
Conditioning
Control
DT-αChnKO
100 μm
c-Fos positive cells
30
25
20
15
10
5
0
**
n=10
n=20
n=13
n=17
Homecage
Conditioning
DT-αChnKO
Control

Figure S3. Altered c-Fos protein expression in the dorsal hippocampus in DT-α2KO mice after fear conditioning

DT-αChnKO mice displayed significantly decreased c-Fos positive cells compared with their control mice in hippocampal CA1 region after conditioning (**p<0.01), but not in homecage (p=0.12).

Figure S4

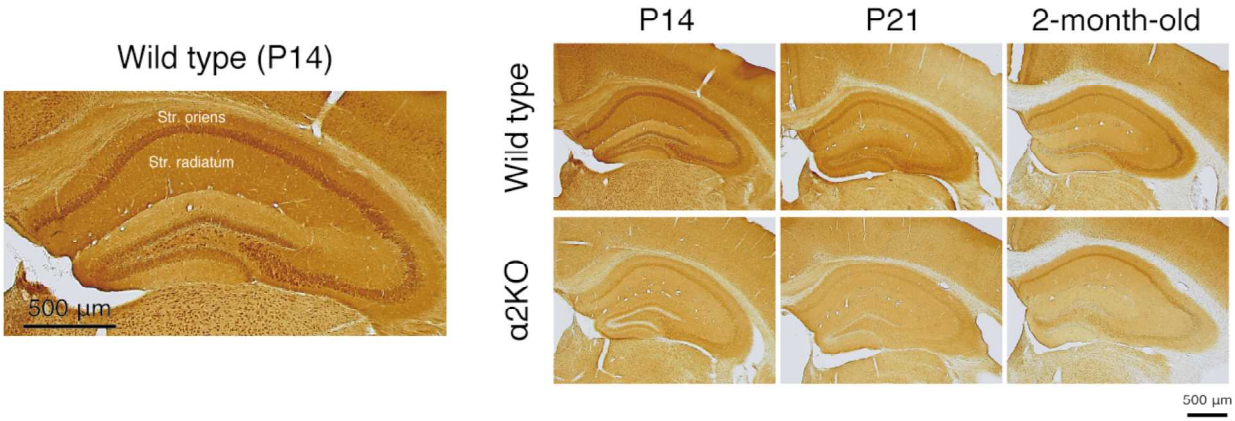
Wild type (P14)
Str. oriens
Str. radiatum
500 µm
P14
P21
2-month-old
Wild type
α2KO
500 µm

Figure S4. α2-chimaerin protein expression pattern in the hippocampus during development

α2-chimaerin expression levels were highest in the stratum radiatum, the pyramidal layer and the stratum oriens of the CA1 region in the hippocampus during development. Scale bar, 500 μm.

Figure S5

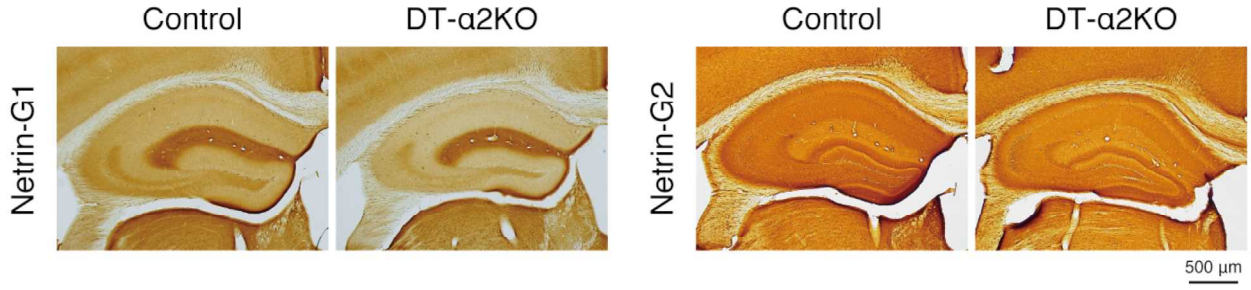

Figure S5. Hippocampal laminar structure appears normal in adult DT-α2KO mice

Immunostaining patterns of netrin-G1 and netrin-G2. Adult DT-α2KO mice showed normal Netrin-G1 and Netrin-G2 protein expression pattern. Scale bar, 500 μm.

Figure S6

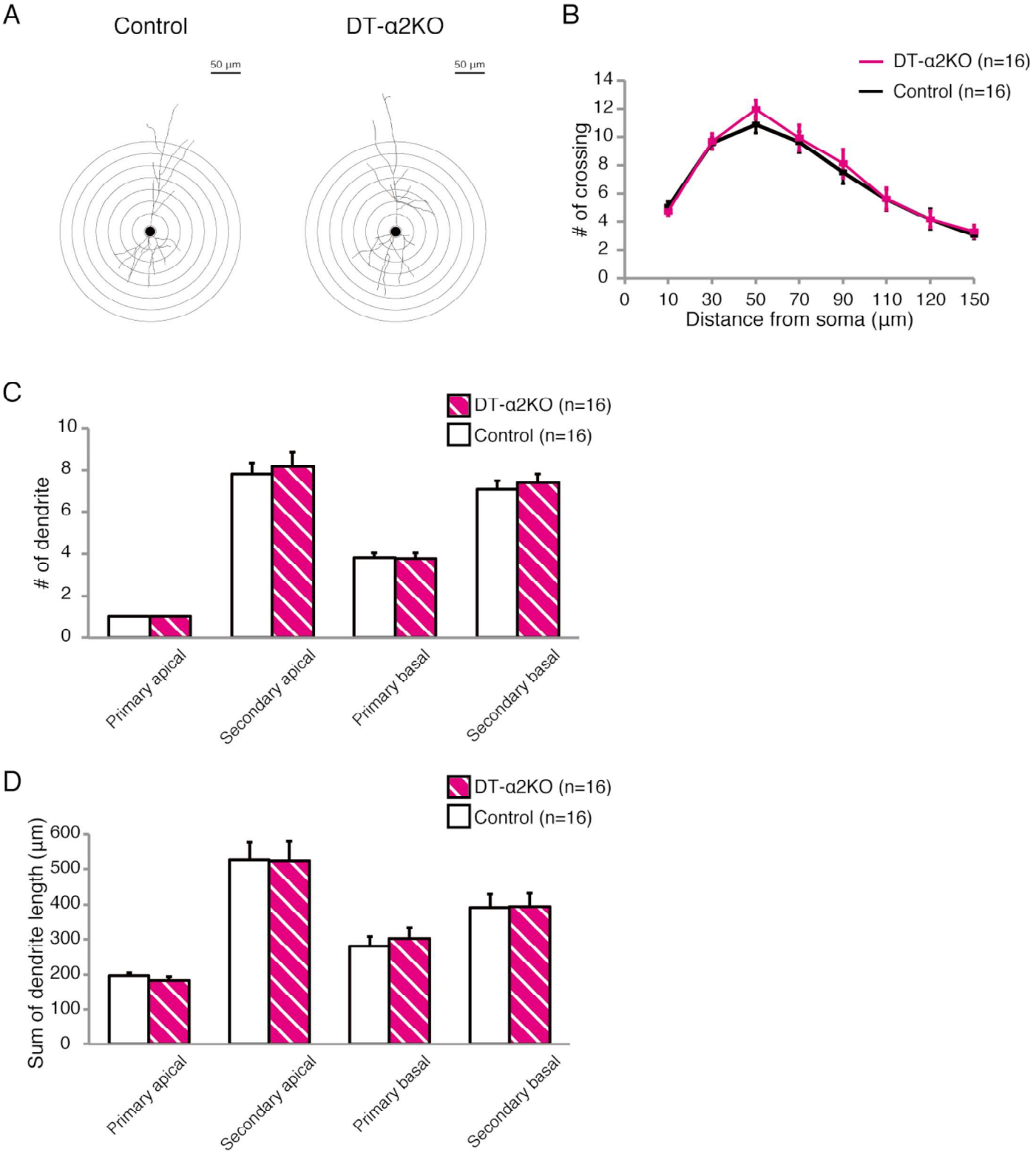
A
Control
DT-α2KO
50 μm
50 μm
B
DT-α2KO (n=16)
Control (n=16)
# of crossing
Distance from soma (μm)
C
DT-α2KO (n=16)
Control (n=16)
# of dendrite
Primary apical
Secondary apical
Primary basal
Secondary basal
D
DT-α2KO (n=16)
Control (n=16)
Sum of dendrite length (μm)
Primary apical
Secondary apical
Primary basal
Secondary basal

Figure S6. Normal dendrite length and complexity of hippocampal CA1 pyramidal neuron in DT-α2KO mice

(A) Representative trace of Golgi-cox-stained neurons from CA1 region of the hippocampus. Scale bar, 50 μm.

(B) Scholl analysis of CA1 pyramidal neuron in DT-α2KO and control mice showed no significant differences in branching patterns throughout the dendritic trees (two-way ANOVA; $F_{(1,30)}$=0.19, p=0.67 for genotype).

(C) Dendrite number is not significantly different between genotypes (Secondary apical: p=0.67, Primary basal: p=0.87, Secondary basal: p=0.59).

(D) Summed dendrite length is not significantly different between genotypes (Primary apical: p=0.41, Secondary apical: p=0.97, Primary basal: p=0.61, Secondary basal: p=0.95). Data are shown as mean±SEM.

Figure S7

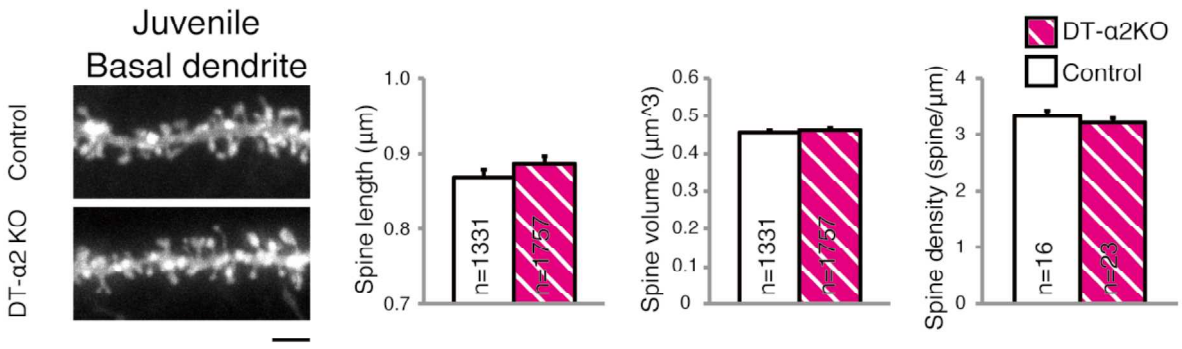
Juvenile
Basal dendrite
Control
DT-α2 KO
Spine length (μm)
1.0
0.9
0.8
0.7
n=1331
n=1757
Spine volume (μm^3)
0.6
0.5
0.4
0.3
0.2
0.1
0
n=1331
n=1757
Spine density (spine/μm)
4
3
2
1
0
n=16
n=23
DT-α2KO
Control

Figure S7. Deletion of α2-cimaerin does not affect spine size and density of basal dendrites in hippocampal CA1 pyramidal neurons

Representative images of DiI-labeled basal dendrites of hippocampal CA1 cells from DT-α2KO mice and their control mice in juvenile (P22-P23). Juvenile DT-α2KO mice showed normal spine morphology and density. There were no significant difference between DT-α2KO mice and their control mice (Spine length: p=0.30, Spine volume: p=0.57, Spine density: p=0.33). Spine length and spine volume3: Mann-Whitney U-test. Scale bar, 2 μm. Data are shown as mean±SEM.

Figure S8

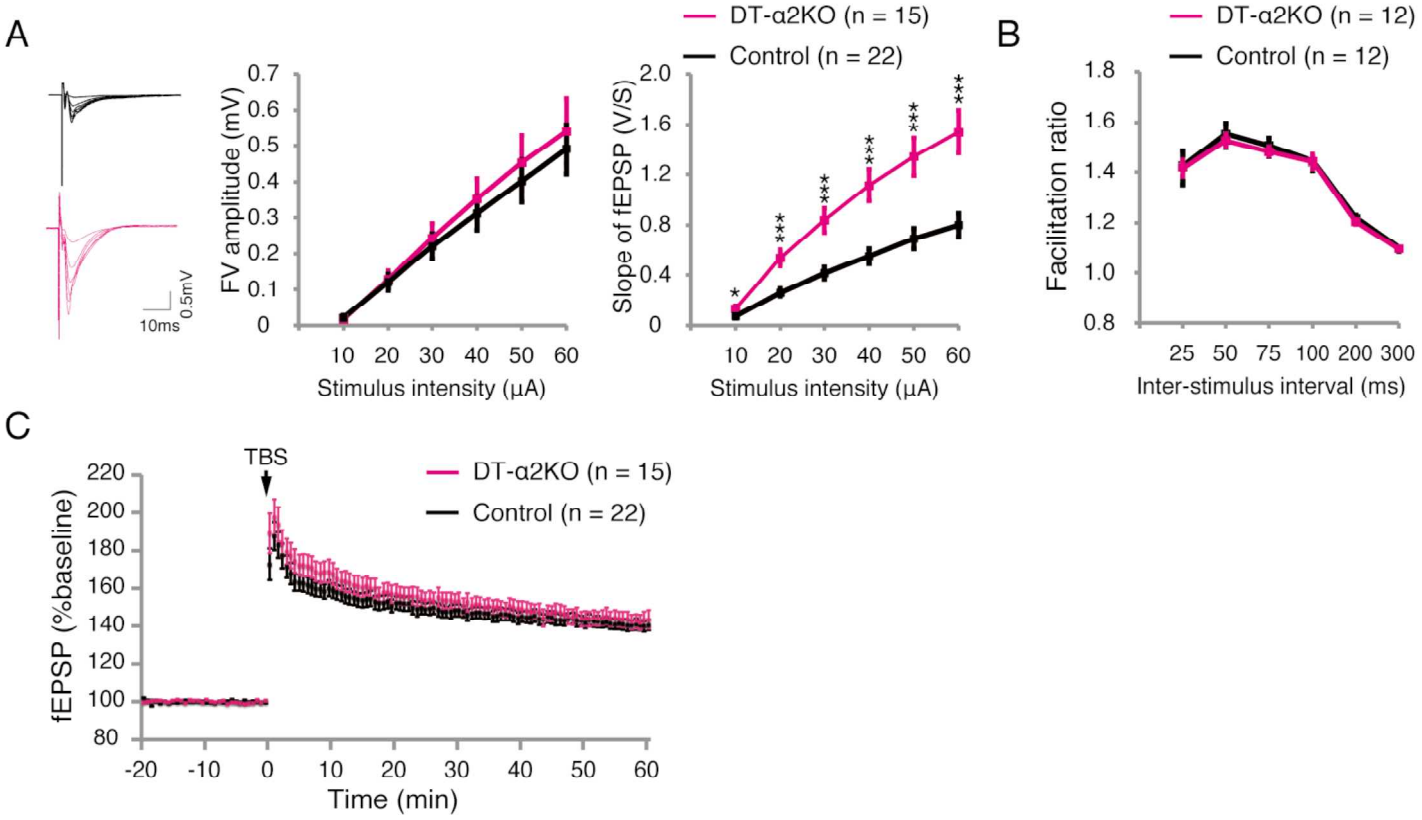
A
10ms
0.5mV
FV amplitude (mV)
Stimulus intensity (μA)
DT-α2KO (n = 15)
Control (n = 22)
Slope of fEPSP (V/S)
Stimulus intensity (μA)
B
DT-α2KO (n = 12)
Control (n = 12)
Facilitation ratio
Inter-stimulus interval (ms)
C
TBS
DT-α2KO (n = 15)
Control (n = 22)
fEPSP (%baseline)
Time (min)

Figure S8. Basal synaptic transmission is increased in the CA3-CA1 pathway of hippocampal slice from DT-α2KO mice

(A) Input-output relation. Representative traces of field potentials recorded in the stratum radiatum of the CA1 region in response to electrical stimulation. The slope of excitatory postsynaptic potential (fEPSP) as a function of stimulus intensity (10 μA to 60 μA) was significantly different between adult DT-α2KO and their littermate control mice (two-way ANOVA; $F_{(1,35)}$=17.88, ***p<0.001 for genotype, $F_{(5,175)}$=16.32, ***p<0.001 for genotype x intensity, Tukey-Kramer post hoc test; *p<0.05, ***p<0.001) without change in the amplitude of presynaptic fiber volley (FV)(two-way ANOVA; $F_{(1,35)}$=0.21, p=0.65 for genotype).

(B) Presynaptic facilitation induced by paired-stimuli, with the intervals of 25 ms, to 300 ms, was not significantly different between DT-α2KO and their control mice (two-way ANOVA; $F_{(1,22)}$=0.038, p=0.84 for genotype).

All spine data were from apical dendrites of CA1 pyramidal neurons. Data are shown as mean±SEM. Scale bars: 100 μm(A); 2 μm(B,D,G).

(C) LTP induced by theta burst stimulation (TBS;15 bursts at 5 Hz, 4 pulses at 100 Hz per each burst) as percent of baseline (-20 to 0 min). No difference in the magnitude of LTP was observed between genotype (averaged last 5 min data; Control: 140.8±2.7%, DT-α2KO: 143.2±4.1%, p=0.61). Data are shown as mean±SEM.

Figure S9

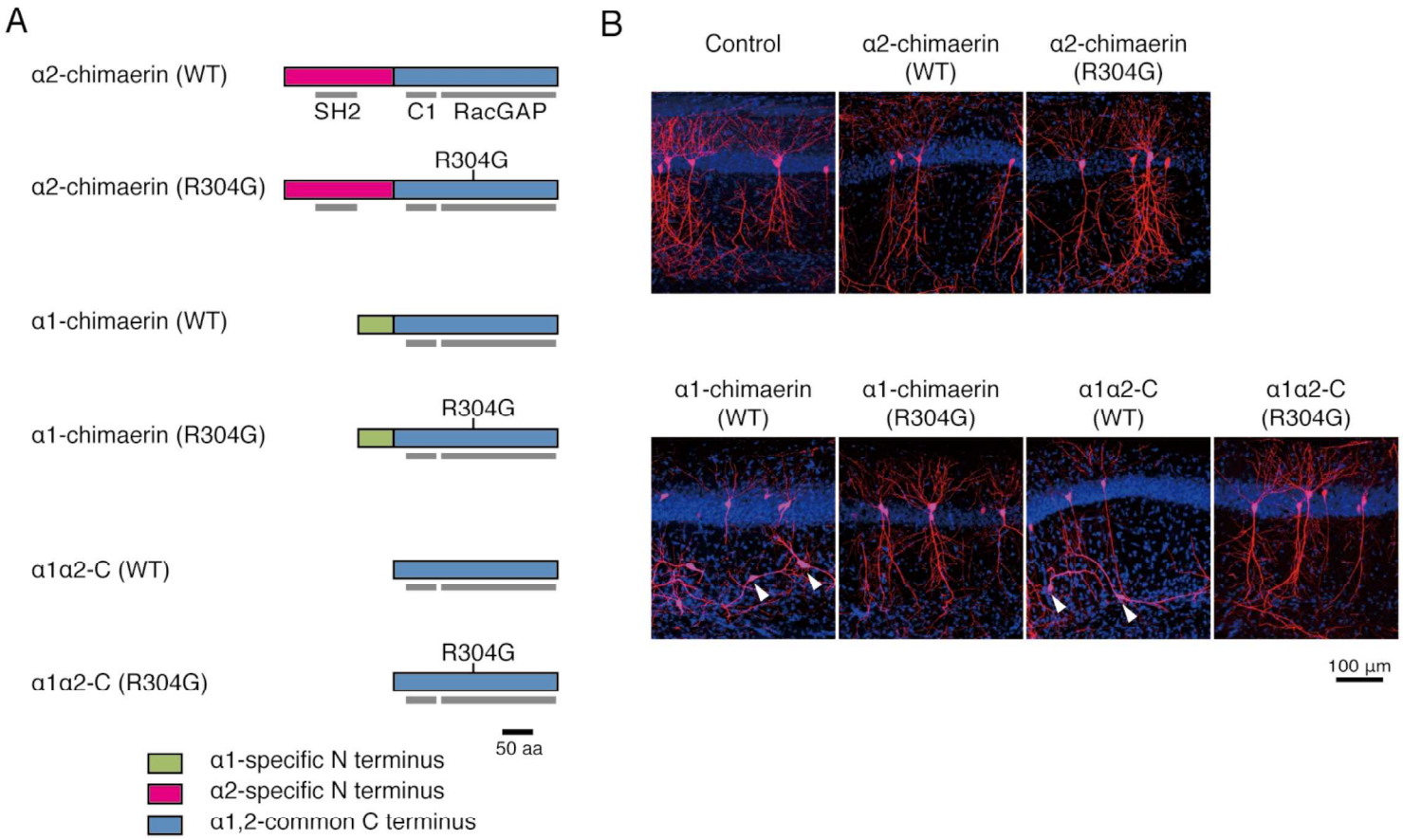
A
α2-chimaerin (WT)
SH2
C1
RacGAP
α2-chimaerin (R304G)
R304G
α1-chimaerin (WT)
α1-chimaerin (R304G)
R304G
α1α2-C (WT)
α1α2-C (R304G)
R304G
50 aa
α1-specific N terminus
α2-specific N terminus
α1,2-common C terminus
B
Control
α2-chimaerin (WT)
α2-chimaerin (R304G)
α1-chimaerin (WT)
α1-chimaerin (R304G)
α1α2-C (WT)
α1α2-C (R304G)
100 μm

Figure S9. Importance of α2-chimaerin-specific N-terminus in the regulation of the RacGAP activity of α-chimaerin

(A) Schematic representation of expression constructs. Each of these proteins fused to monomeric RFP in their C-terminal regions.

(B) CA1 pyramidal neurons from juvenile (P22-P23) WT mice expressing RFP alone (Control), or RFP and α-chimaerin proteins. Neurons expressing α2-chimaerin (WT) or RacGAP-inactive α2-chimaerin (R304G) were located in the pyramidal layer of CA1. On the other hand, expression of either α1-chimaerin or

(α1α2-C) affected cell migration. Some neurons exhibited irregular shape and position in CA1 region (arrow head). These abnormalities were not observed in RacGAP-inactive mutant (R304G)-expressing neurons. Blue color indicated DAPI signal. Scale bar, 100 μm.

Figure S10

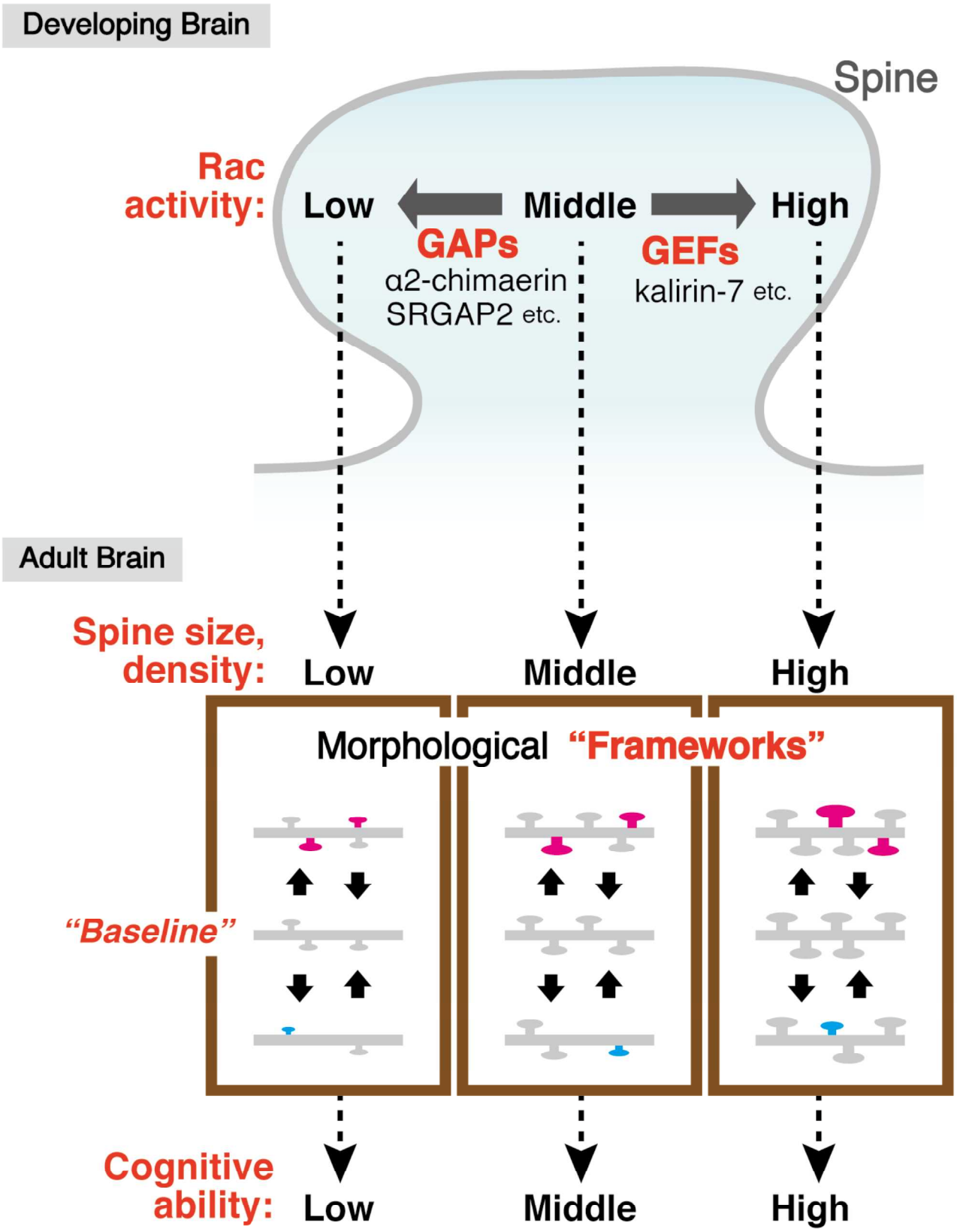
Developing Brain
Spine
Rac activity:
Low
Middle
High
GAPs
α2-chimaerin
SRGAP2 etc.
GEFs
kalirin-7 etc.
Adult Brain
Spine size, density:
Low
Middle
High
Morphological "Frameworks"
"Baseline"
Cognitive ability:
Low
Middle
High

Figure S10. A model for the developmental adjustment of the "baseline and framework" of spine morphology, which underlie cognitive ability

Rac activity levels of the dendritic spine in the developing brain, which are determined by a balance between RacGEF (e.g., Kalirin-7)-mediated activation and RacGAP (e.g., α2-chimaerin and SRGAP2)-mediated inactivation, adjust the "baseline and framework" of spine morphology (e.g., size and density) in adulthood; and thereby adjust the cognitive ability. Increased Rac activity in development leads to an increased baseline, and thereby increases cognitive ability. On the other hands, decreased Rac activity in development leads to decreased baseline, and thereby decreases cognitive ability. This model may also explain the difference of cognitive ability between species (e.g., humans and mice).

SUPPLEMENTAL EXPERIMENTAL PROCEDURES

New Mouse Lines Used in This Study

The αChn-flox (with pgk-neo) allele, in which a loxP was inserted into a *Kpn*I site upstream of Exon 9 and an FRT-pgk-neo-FRT-loxP cassette was inserted into the *Hind*III site downstream of Exon 10, was generated by homologous recombination in ES cells; the targeting vector was constructed by restriction enzyme digestion and ligation. The α1-flox (with pgk-neo) allele, in which an FRT-pgk-neo-FRT-loxP cassette was inserted into the *Psh*AI site about 2.5 kb upstream of transcriptional initiation site of the α1-chimaerin gene and a loxP was inserted into the *Xho*I site in the 5' untranslated region of the α1-chimaerin gene in exon 7, was generated by homologous recombination in ES cells; the targeting vector was constructed mostly by restriction enzyme digestion and ligation. The α2-flox allele (with pgk-neo) allele, in which an FRT-pgk-neo-FRT-loxP cassette was inserted into a locus about 500 bp upstream of exon 6 and a loxP was inserted into a locus 500 bp downstream of exon 6, was generated by homologous recombination in ES cells; the targeting vector was constructed by modifying a bacterial artificial chromosome clone RP23-271L22 by homologous recombination in *E.coli* using the Red/ET recombination system (Gene Bridges). All of these lines of mice were generated by using MS12 ES cells derived from B6 strain (Kawase et al., 1994) and maintained in a B6 genetic background. To generate the αChn-flox, α1-flox and α2-flox alleles, the pgk-neo selection marker franked by a pair of FRTs was removed from the germline by crossing these mice with CAG-FLPe deleter mice (Kanki et al., 2006). The α1KO and α2KO alleles were generated by inducing Cre-mediated recombination in germline of α1-flox and α2-flox mice, respectively.

Mouse Lines and Genotyping

αChnKO (Iwasato et al., 2007), Emx1Cre KI-ΔNeo (Iwasato et al., 2000; Iwasato et al., 2008) and SLICK-H transgenic (Young et al., 2008) mice were previously reported. PCR primer pairs for genotyping are as follows: 5'-GGAGTTCCAGCTCCATTGTG-3' / 5'-CAAGGAAAGCCCTCCAGATG-3' (137 bp, 184 bp and no bands for WT, αChn-flox and αChnKO alleles, respectively); 5'-GTACACTAGGATCTCAGCTC-3' / 5'-TCAGCTAGCACATGAGCATG-3' (360 bp for α1KO allele); 5'-GTACACTAGGATCTCAGCTC-3' / 5'- AGCTTGGGTAGTAACAAGAC-3' (471 bp and 583 bp bands for WT and α1-flox alleles, respectively); 5'-ATGCAGTAGCACACTTCAGC-3' / 5'-AGTGCTGGCCTTTAAGTATG-3' (421 bp and 1.6 kb bands for α2KO and WT alleles, respectively); 5'-ATGCAGTAGCACACTTCAGC-3' / 5'-AACTATCACACTGTTATGAG-3' (328 bp and 408 bp bands for WT and α2-flox alleles, respectively); 5'-ACCTGATGGACATGTTCAGGGATCG-3' / 5'-TCCGGTTATTCAACTTGCACCATGC-3' (108 bp band for Emx1Cre KI-ΔNeo and SLICK-H).